



Norwegian University of
Science and Technology

Design of Composite Wing Kite

Sigrid Moen

Materials Science and Engineering

Submission date: June 2016

Supervisor: Nils Petter Vedvik, IPM

Norwegian University of Science and Technology
Department of Engineering Design and Materials

NTNU - NORWEGIAN UNIVERSITY
OF SCIENCE AND TECHNOLOGY
DEPARTMENT OF ENGINEERING DESIGN
AND MATERIALS

**MASTER THESIS SPRING 2016
FOR
STUD. TECHN. SIGRID MOEN**

Design of Composite Wing Kite

Kitemill develops a wing kite for energy generation. The wing is constructed as a plane supported to a winch and a generator at the ground. 80% of the time the generator produces energy, and the remaining 20%, the kite is pulled back to the starting point. When the kite is attached of the wind, it enters a helical path, until maximum extension of the tether is reached. To produce energy, the tether slows down the pull force of the kite. The kite returns to the ground station through a straight line. Then the whole process starts over again and could possibly continue for a long time.

The wing of the kite shall be assembled of two symmetrical components due to manufacturing and transport issues. An optimized joiner connecting the two wing halves shall be designed in this master project work.

The design will involve carbon fiber composites and design process shall include both an FEA analysis and development of manufacturing process using pre-preg materials.

Previous specialization project thesis by the candidate serves as extended background to the current master project work.

Formal requirements:


Three weeks after start of the thesis work, an A3 sheet illustrating the work is to be handed in. A template for this presentation is available on the IPM's web site (see <https://www.ntnu.edu/web/ipm/master-thesis>). This sheet should be updated one week before the master's thesis is submitted.

Risk assessment of experimental activities shall always be performed. Experimental work defined in the problem description shall be planned and risk assessed up-front and within 3 weeks after receiving the problem text. Any specific experimental activities which are not properly covered by the general risk assessment shall be particularly assessed before performing the experimental work. Risk assessments should be signed by the supervisor and copies shall be included in the appendix of the thesis.

The thesis should include the signed problem text, and be written as a research report with summary both in English and Norwegian, conclusion, literature references, table of contents, etc. During preparation of the text, the candidate should make efforts to create a well arranged and well written report. To ease the evaluation of the thesis, it is important to cross-reference text, tables and figures. For evaluation of the work a thorough discussion of results is appreciated.

The thesis shall be submitted electronically via DAIM, NTNU's system for Digital Archiving and Submission of Master's theses.

The contact person is Tor Sigurd Breivik, Kongsberg Defense and Aerospace



Torgeir Welo
Head of Division



Nils Petter Vedvik
Professor/Supervisor



NTNU
Norges teknisk-
naturvitenskapelige universitet
Institutt for produktutvikling
og materialer

Abstract

New methods to produce environmentally-friendly energy, is a growing technology area. By using wind at high altitudes, Kitemill wants to be a part of this revolution. Operations in the air requires high quality and security of components. Furthermore, rough conditions make demands on excellent material properties. For this purpose carbon fiber composite is suited for use. This is one of the areas of expertise at Kongsberg Defence Systems (KDS), and it is in their interest to develop new utilization for the technology. Kitemill's concept is based on a plane consisting of a wing, divided into two separate parts. To connect the two halves, a joiner is needed. During this master work design, manufacturing process and production of an optimized joiner, together with a finite element analysis (FEA), has been the main focus.

Two different designs for the joiner have been evaluated, a rectangular box profile and an I-beam with foam core. A manufacturing process for the two profiles were developed, using Kitemill's existing mold tool as base. During the layup of the two joiners, differences and experiences were detected to discuss further improvement of the manufacturing process. A four point bending test were performed to test the two manufactured joiners. The results from the bending test were verified through a FEA analysis, and the results corresponded well. Furthermore, a buckling analysis were performed, and confirmed that failure due to buckling will not be crucial for the applied loads. Finally, all results and processes were compared, to obtain the most suited design and manufacturing process for the joiner.

The results from experimental work and FEA analysis concluded with the I-beam as the best design for the joiner. Furthermore, some recommendations was given to improve the manufacturing process.

Sammendrag

Utvikling av nye og miljøvennlige metoder for å produsere energi, er et voksende teknologisk område. Mer miljøvennlige produksjonsmetoder er ønskelig for fremtiden. Ved å utnytte vind i høye luftlag, ønsker Kitemill å ta del i denne utviklingen. Operasjoner i lufta krever komponenter av høy kavlitet og sikkerhet. Videre gjør de krevende omgivelsene at det stilles høye krav til komponentenes materialegenskaper. Dette gjør karbon fiber kompositt svært egnet, og dette er et område hvor Kongsberg Defence Systems (KDS) har høy ekspertise. Nye anvendelser av denne teknologien står i deres søkelys, noe som gjør Kitemill til et spennende konsept. Dette baserer seg på et fly, som har en vinge som skal være delbar. For å kunne binde de to vingehalvdelenene sammen, trengs det en joiner. I denne masteroppgaven er det design, produksjonsmetode og produksjon av en optimalisert joiner, sammen med en element analyse, som har stått i fokus.

To ulike design for joineren har blitt evaluert, en rektangulær hul boks og en I-bjelke med skumkjerne. En produksjonsmetode for de to profilene, ble utviklet ved å ta utgangspunkt i Kitemills eksisterende støpeverktøy. Erfaringer og forskjeller mellom de to profilene ble evaluert og diskutert underveis i produksjonen for å finne mulige forbedringsområder. De to produserte joinerne ble testet i en firepunkts bøyetest. Resultatene fra denne, ble verifisert og sammenlignet med resultatene fra elementanalysen, og disse korresponderte bra. Det ble også gjort en simulering av knekking, og denne beviste at knekking ikke vil være kritisk for den maksimale påførte lasten. Tilslutt ble alle prosesser og resultater sammenlignet, for å konkludere med det beste designet og den beste produksjonsprosessen for joineren.

Resultatene fra det eksperimentelle arbeidet og simuleringen, konkluderer med at det er I-bjelken som vil være det beste designet for joineren. I tillegg er det foreslått noen tiltak som vil gjøre produksjonsmetoden utviklet under dette arbeidet enda bedre.

Preface

This thesis is written as the final work to complete the degree Master of Science in Materials Science and Engineering. It is written at the Department of Engineering Design and Materials at Norwegian University of Science and Technology (NTNU), in cooperation with Kongsberg Defence Systems (KDS). The master work has been carried out during spring 2016, as a continuation of a specialization project, during fall 2015.

The idea to the assignment was brought up during my summer internship at KDS, at the division Aerostructures, summer 2015. Kitemill is related to KDS through Kongsberg Innovasjon, and requested support for research on a joiner for their wing kite system. This appeared to be a great subject for a specialization project followed by a master thesis, and the assignment was made.

Trondheim, June 8, 2016

Sigrid Moen

Sigrid Moen

Acknowledgment

I would like to thank KDS for giving me the opportunity to write this master thesis. A special thanks to my supervisor at KDS, Tor Sigurd Breivik, for all his support and answers to my questions. I am also grateful for all the help and counsellings from my supervisors at NTNU, Associate Professor Nils Petter Vedvik and Professor Andreas Echtermeyer.

The employees in the lay-up- and demolding laboratories, at KDS division Aerostructures, also deserves a great thanks for all their good advices and assistance during production of joiners. A special thanks to Lars Kristiansen, Heidi Bakke, Åse Teksle, Freddy Knutsen and Jean-David Holmes for their huge excitement and interest in my work. Carl-Magnus Midtbø and Børge Holen in the Mechanical testing lab at IPM NTNU also deserves a thank, for their help during milling of the mould and mechanical testing of the joiners.

Thanks also to Sture Smidt in Kitemill for his help with questions directly related to Kitemill and their concept. The rest of the Kitemill team also deserves my gratitude for letting me visit their facilities at Lista, to see how they work.

S.M.

Contents

Abstract	i
Sammendrag	iii
Preface	v
Acknowledgment	vii
List of Figures	xii
List of Tables	xiv
Nomenclature	xv
1 Introduction	1
1.1 Background and motivation	1
1.2 Structure of thesis	4
1.3 Limitations	5
2 Theory	7
2.1 Laminate theory	7
2.2 Bending	10
2.2.1 Bending test	12
2.3 Buckling analysis	13
3 Preliminaries	15
3.1 Models and requirements	15
3.2 Material properties	16
3.3 Layup sequence	18
3.4 Theoretical laminate properties	19
3.5 Prototype production	20

4 Experimental Work	23
4.1 Molds	23
4.2 Layup	26
4.2.1 Rectangular box profile	26
4.2.2 I-beam	29
4.3 Demolding	33
4.4 Results	34
4.5 Testing of components	36
4.5.1 Results	38
5 FE-Analysis	43
5.1 Imperfections	43
5.2 Model calibration	45
5.2.1 Geometries	45
5.2.2 Materials	46
5.2.3 Loads and boundary conditions	48
5.2.4 Mesh	49
5.3 Four point bending test	51
5.3.1 Results	51
5.4 Buckling analysis	54
5.4.1 Results	54
6 Discussion	57
6.1 Comparison of theoretical and practical results	57
6.2 Profile evaluation	61
6.3 Improvement of manufacturing process	62
7 Conclusion	65
8 Further Work	67
Bibliography	68

<i>CONTENTS</i>	xi
A Machine Drawings for Mold	73
B Matlab Code	79
C Calculations after four point bending test	85
C.1 Rectangular box profile	86
C.2 I-beam	87
D Risk Assessment	89

List of Figures

1.1	Kitemill's concept	1
1.2	The energy generating process	3
2.1	Definitions of laminate and ply	7
2.2	Bending moment	11
2.3	Four point bending test	13
3.1	Geometries of models	15
3.2	Joiner as produced today	21
4.1	Mold base	24
4.2	Technique used for layup of the rectangular box profile	25
4.3	Technique used for layup of the I-beam	25
4.4	Step 1 layup of first ply of the rectangular box profile	26
4.5	Step 2 of layup for the rectangular box profile	27
4.6	Step 3 of layup for the rectangular box profile	28
4.7	Top of mold inserted	28
4.8	Bagging of the rectangular box profile	29
4.9	Step 1 of layup for the I-beam	30
4.10	Step 2 of layup for the I-beam	31
4.11	Step 3 of layup for the I-beam	31
4.12	Bagging of I-beam	32
4.13	Demold, after autoclave	33
4.14	Finished joiners	34
4.15	Schematic view of test setup	36
4.16	Test setup for four point bending test at IPM NTNU	37
4.17	Results after four point bending test for the rectangular box profile	38
4.18	Results after four point bending test for the I-beam profile	39
4.19	Displacement curves for rectangular box profile	40

4.20 Displacement curves for I-beam	41
5.1 Difference between continuum and conventional shell elements	44
5.2 Geometry for the rectangular box profile	45
5.3 Geometry for the I-beam	46
5.4 Loads and boundary conditions	48
5.5 Elements used in the analysis	50
5.6 Mesh details for rectangular box profile	50
5.7 Mesh details for I-beam	50
5.8 Results from four point bending test for rectangular box profile	52
5.9 Displacement curve of analytical results for rectangular box profile	52
5.10 Results from four point bending test for I-beam	53
5.11 Displacement curve of analytical results for I-beam	53
5.12 Results of buckling analysis for rectangular box profile	55
5.13 Results of buckling analysis for I-beam	55
A.1 Bottom of mold	74
A.2 Top of mold	75
A.3 Inside block for rectangular box profile	76
A.4 Inside blocks for I-beam	77
C.1 Free body diagram	85
C.2 Geometric dimensions	85

List of Tables

3.1	Preliminary thicknesses	16
3.2	Material properties for HexPly 8552 5HS	17
3.3	Material properties for Rohacell 110 Rist-HT 0.005 mm	17
3.4	Layup calculations	19
3.5	Calculated layup sequences	19
3.6	Theoretical laminate properties	20
3.7	Theoretical weight	20
4.1	Measured length and weight of the produced parts	34
4.2	Measured thicknesses of the produced parts, top and bottom	35
4.3	Measured thicknesses of the produced parts, sides	35
4.4	Comparison of tensile modulus	42
5.1	Material properties for HexPly 8552 5HS used in the analysis	47
5.2	Material properties for Rohacell used in the analysis	47
6.1	Comparison of theoretical and experimental results	57

Nomenclature

A_{ij}	In plane stiffness matrix	S_{xy}	In-plane shear strength
B_{ij}	Bending-extension coupling matrix	S_{yz}	Out-of-plane shear strength
CPT	Cured ply thickness	t_k	Thickness of ply
D_{ij}	Bending stiffness matrix	v^M	Nontrivial displacement solutions
E_x	Tensile modulus longitudinal direction	X_C	Compression strength in longitudinal direction
E_y	Tensile modulus transverse direction	X_T	Tensile strength in longitudinal direction
E_z	Tensile modulus out-of-plane direction	y	Distance from neutral axis
\overline{EI}	Bending stiffness	Y_C	Compression strength in transverse direction
FEA	Finite element analysis	Y_T	Tensile strength in transverse direction
G_{xy}	In-plane shear moduli	\bar{z}_k	Coordinate of the middle surface of the k th ply
G_{xz}	Through thickness shear moduli	ϵ	Strain
G_{yz}	Out-of-plane shear moduli	κ	Radius of curvature
I	Moment of inertia	λ_i	Eigenvalues
\mathbf{K}^{MN}	Tangent stiffness matrix	ν	Poisson's ratio
\mathbf{K}_0^{MN}	Material stiffness matrix	ρ	Density
\mathbf{K}_Δ^{MN}	Geometric stiffness matrix	σ_{ax}	Axial stress
KDS	Kongsberg Defence Systems	$\sigma_{Bend.}$	Bending stress
M	Moment		
$(\bar{Q}_{ij})_k$	Coefficients in laminate coordinates of the plane-stress stiffness matrix		

1. Introduction

1.1 Background and motivation

Kitemill is a newly established Norwegian energy producing company. Their concept is to utilize wind at high altitudes to generate energy. The system is based on a plane, coupled to a winch and a generator at the ground, as illustrated in Figure 1.1 [1]. Today new and more environmentally-friendly methods for energy production is a growing area. Kitemill wants to be a part of this revolution, and their vision is to utilize the stable winds at high altitudes. Together with creating stations that are less visible in the landscape than more traditional systems, e.g. windmills [1].

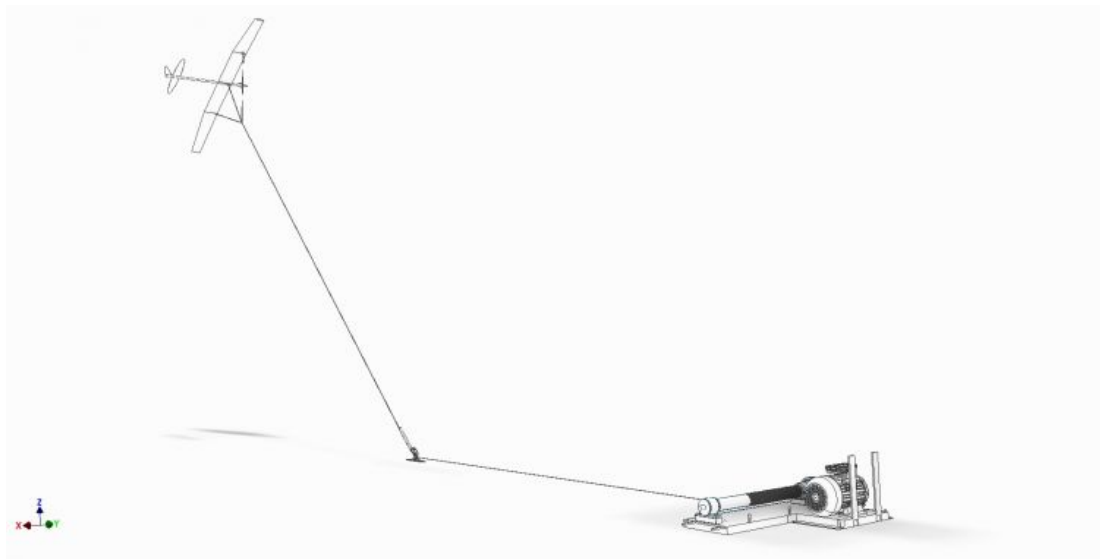


Figure 1.1: Kitemill's concept [1]

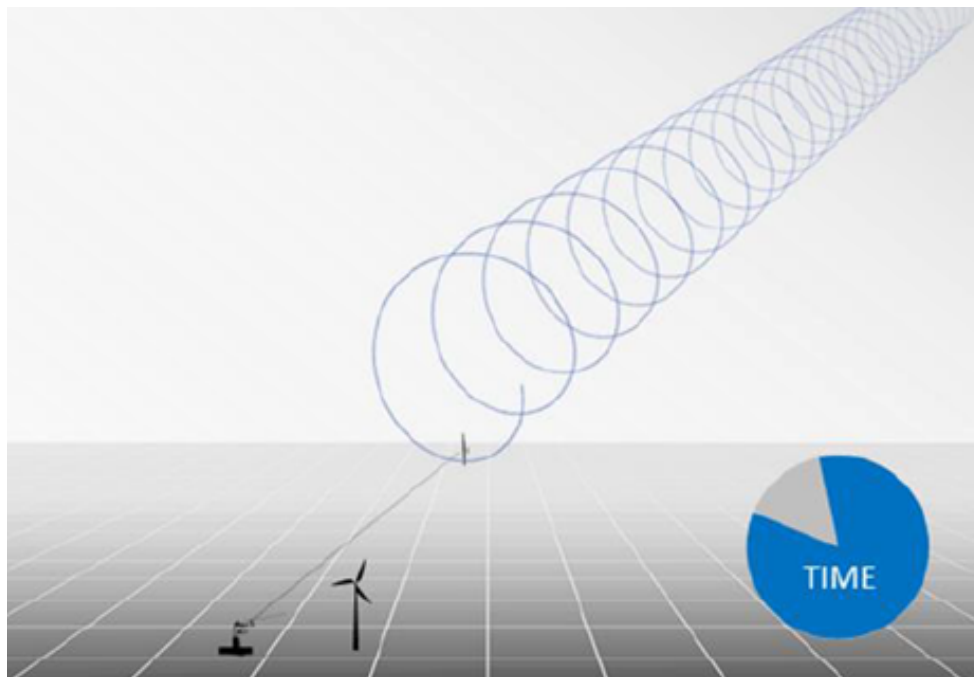
Kongsberg Defence Systems (KDS), and their division Aerostructures, is a leading company producing composites for the aerospace industry. It is in their interest to develop new applications for the technology, where their expertise and experience in the field can be fully exploited. This, together with a need of recruitment, elevate their willingness to support competence development, at the composite field in Norway. Companies in the technology

park at Kongsberg created Kongsberg Innovasjon to help entrepreneurs and small businesses with industrial partners. Kitemill is part-owned and part-financed by Kongsberg Innovasjon. This relates Kitemill and KDS, which means that KDS contributes with competence and experience in the composite field, to Kitemill's advantage.

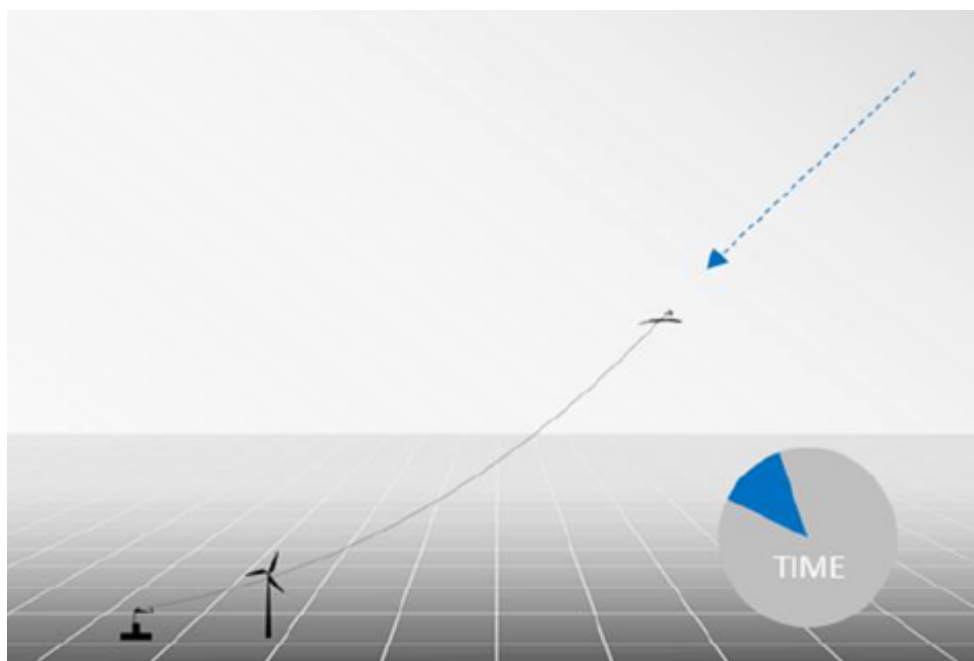
The general principle of Kitemill's concept is that 80% of the time the turbine at the ground station produces energy. The remaining 20% of the time the kite is pulled back to the starting point, as illustrated in Figure 1.2. The kite is attached to the wind, and enters a helical path until maximum extension of tether is reached. To produce energy the tether slows down the pull force of the kite. When the tether is completely extended, the angle of the kite relative to the tether is modified. Then the kite turns to the ground station through a straight line. The process continues, and the same procedure could possibly be repeated for a long time.

The kite in the system is similar to a plane, and consist of two wings which both are assembled in two separate parts, due to production and transporting issues. An optimized joiner is needed to connect the two parts together, and during the master work this joiner is to be produced in two different versions. Testing of two different profiles against each other, and developing an efficient manufacturing process, are the focus areas of this master work.

The specialization project [2] discusses different materials and geometries for use in the joiner. It concluded with a material of carbon fiber composite, together with a construction formed as a rectangular box profile or an I-beam. Furthermore, it was suggested to use a core of foam to further stabilize and strengthen the part. In light of this discussion it is decided to continue with a rectangular box profile and an I-beam in the master work. The rectangular box profile will be hollow, while a core will be inserted in the middle of the I-beam. This will make it possible to conclude with the most optimized design and manufacturing process.



(a) Helical path



(b) Returing path

Figure 1.2: The energy generating process [1]

1.2 Structure of thesis

Chapter 1: Introduction

The introduction presents the background and motivation for the master work.

Chapter 2: Theory

Relevant theory for the experimental and analytical work in the thesis is presented. Topics include laminate theory, bending- and buckling analysis.

Chapter 3: Preliminaries

This chapter includes calculations and preparations done before any experimental or analytical work started. This was done to ensure that all parameters, regarding material properties and geometries of the model, were similar for both cases. This will make the results comparable at a later stage.

Chapter 4: Experimental

This chapter explains how the experimental work was performed, including both manufacturing processes and testing of parts.

Chapter 5: FE-analysis

The chapter consists of an explanation of how the FE-analysis was performed, together with a discussion of which type of simulation that will be most appropriate for comparison with the experimental work. Detailed descriptions of how the FE-analysis in Abaqus was developed, together with the results, are presented.

Chapter 6: Discussion

This chapter discusses the results obtained during experimental and analytical work. A comparison of the results and a related discussion of them are performed. Furthermore, the manufacturing processes are evaluated and discussed in detail, to find possible improvements for future mass production.

Chapter 7: Conclusion

This chapter presents the conclusion of the results of the master work.

Chapter 8: Further Work

Recommendations for further work is presented in this chapter.

1.3 Limitations

The scope of the master work is limited to two different profiles, one rectangular box profile and an I-beam. The rectangular box profile is hollow, while a core is inserted inside the I-beam. This makes it possible to analyze both the difference between the two profiles, together with use of a core for further stabilization. Furthermore, it is decided to use prepreg as production process for both joiners. The limitation to one manufacturing process is based on that prepreg is the area of expertise at KDS. It is therefore desirable to develop a production method that could be used at KDS for Kitemill in the future. Compared to the geometric dimensions in the specialization project, height and width of the joiner are changed. Some adjustments to the calculations and results are done to make the results adaptable to the master work.

2. Theory

Design of a component requires an understanding of the theory behind material properties, and how this is correlated to a components behaviour. For composite materials, laminate theory relates properties to behaviour of the finished component. Moreover, to qualify the design it is significant with an understanding of mechanical behaviour of components, and how this could be used to test if the component fulfill the requirements. In this chapter, theory behind concepts used in both experimental and analytical work is presented.

2.1 Laminate theory

Laminated composites are the structure and properties that results when multiple layers of fibers and resin are assembled. The combination of orientations, thicknesses and materials, results in a layup sequence that forms the wanted product together with its properties. In this thesis a ply refers to one layer or physical sheet of material, i.e. the layup or laminate consists of multiple plies, as illustrated in Figure 2.1. The orientation of a laminate is relative to the x-axis, which means that the 0° -direction is defined as the direction parallel to the x-axis [3].

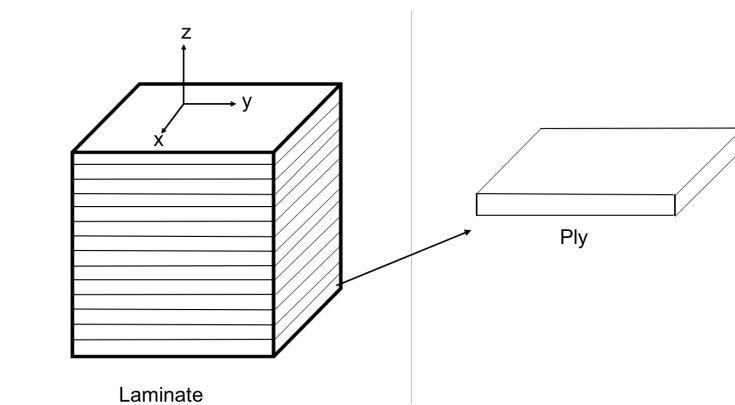


Figure 2.1: Definitions of laminate and ply

To find the relation between forces, stresses and strains throughout the laminate, integrals of the stress components over the thickness could be used. This gives the plate stiffness equation,

as shown in Equation 2.1.

$$\begin{Bmatrix} N_x \\ N_y \\ N_{xy} \\ M_x \\ M_y \\ M_{xy} \end{Bmatrix} = \begin{bmatrix} A_{11} & A_{12} & A_{16} & B_{11} & B_{12} & B_{16} \\ A_{12} & A_{22} & A_{26} & B_{12} & B_{22} & B_{26} \\ A_{16} & A_{26} & A_{66} & B_{16} & B_{26} & B_{66} \\ B_{11} & B_{12} & B_{16} & D_{11} & D_{12} & D_{16} \\ B_{12} & B_{22} & B_{26} & D_{12} & D_{22} & D_{26} \\ B_{16} & B_{26} & B_{66} & D_{16} & D_{26} & D_{66} \end{bmatrix} \begin{Bmatrix} \epsilon_x^0 \\ \epsilon_y^0 \\ \gamma_{xy}^0 \\ \kappa_x \\ \kappa_y \\ \kappa_{xy} \end{Bmatrix} \quad (2.1)$$

Where,

$$A_{ij} = \sum_{k=1}^N (\bar{Q}_{ij})_k t_k; \quad i,j=1,2,6 \quad (2.2)$$

$$B_{ij} = \sum_{k=1}^N (\bar{Q}_{ij})_k t_k \bar{z}_k; \quad i,j=1,2,6 \quad (2.3)$$

$$D_{ij} = \sum_{k=1}^N (\bar{Q}_{ij})_k (t_k \bar{z}_k^2 + \frac{t_k^3}{12}); \quad i,j=1,2,6 \quad (2.4)$$

In equations 2.2-2.4, $(\bar{Q}_{ij})_k$ are the coefficients in laminate coordinates of the plane-stress stiffness matrix, for the respective layer number k , with ply thickness t_k and coordinate of the middle surface of the k th ply, \bar{z}_k [4].

The laminate stiffness matrix contains three sub-matrices, [A], [B] and [D] [5]. For the laminate each sub-matrix represent different properties. The [A] matrix relates the in plane stresses to the inplane forces, and is called the inplane stiffness matrix. This means that obtained matrix [A], could be used to calculate tensile modulus of laminates. This is related as shown in Equation 2.5. In the [B]-matrix, called the bending-extension coupling matrix, inplane strains are related to the bending moments and curvatures to inplane forces. Finally, the [D]-matrix relates the curvatures to the bending moments, and is called the bending stiffness matrix.

$$E_x = \frac{1}{t} \left(A_{xx} - \frac{A_{xy}^2}{A_{yy}} \right) \quad (2.5)$$

By using the equations from above, it is possible to calculate properties for each ply, together with properties for the whole laminate. This means that even though the fibers and resin in a ply, together forms some mechanical properties, they do not reflect the mechanical properties of the constructed laminate or composite component directly. That is what makes the laminate theory calculations important in a design process for structures and components made out of composite materials. The bending stiffness of a laminate is the product of its tensile modulus and moment of inertia. Furthermore, it is related to the moment, height and strain in the laminate, as shown in Equation 2.6.

$$\overline{EI} = \frac{Mh}{2\epsilon} \quad (2.6)$$

Where \overline{EI} represents the sum of the bending stiffnesses of the laminates in the composite section. E.g. for a composite I-beam with two different layup sequences, one for flange and one for web, the bending stiffness for the web and the flange will be different. Which means that \overline{EI} defines the sum of the bending stiffness in the web and both flanges, i.e. the bending stiffness of the I-beam.

Notation and laminate descriptions use matrices, where the value to the left is the first layer, starting from the bottom of the structure. The matrix gives information of the angle of the ply, and if one ply is followed by another ply in the same direction, this is indicated with the number of plies in a subscript. E.g. $[45 -45 0_3]$ indicates that three plies in the 0° -direction should be added after one layer in the 45° -direction and one in -45° -direction. Moreover, for a symmetric laminate only half of the stacking sequence is represented, followed by a subscript, S. These laminates are defined by the same material, thickness and orientation, with respect to the middle surface, throughout the structure [5]. This means that after all the plies in the matrix are added, twice as many layers should follow, starting from the opposite side. The subscript S act as a mirror-plane, and the stacking sequence now starts from right to left.

Symmetric laminates are important to avoid warping. A laminate consisting of the layup sequence [0/45/45/0] is symmetric, as long as the material and thickness is the same, regardless of orientation. Furthermore, balanced laminates refers to laminates with the same amount of plies in each direction, i.e. the layup sequence [45/-45/-45/45].

2.2 Bending

Failure due to material properties, e.g. tensile- and compression strength, is important to evaluate when designing a component. During the specialization project [2], material selection with evaluation of properties were studied. This included calculations of needed bending strength compared to tensile modulus. In this section a short recap of theory behind is repeated. For a structure with moment M , height h , and moment of inertia I , the bending stress is given by Equation 2.7 [5].

$$\sigma_{\text{Bend.}} = \frac{M h}{I} \quad (2.7)$$

When a transverse force is applied to a beam, bending moments arise. This means that at one point of the section, the bending moment corresponds to the applied force times the distance from the section. The internal moments, that arise from the produced stresses, contribute to balance of the bending moment. All the elements of the beam have an internal moment, and by a summation of these, the internal moment for the whole beam is found. This means that the bending moment of a beam can be written as in Equation 2.8.

$$M = \int y(\sigma dA) \quad (2.8)$$

The beam will bend with an angle, θ , related to the start position. Figure 2.2 shows that θ is given by the axial strain, ϵ , divided by the distance from the neutral axis, y . Furthermore, the radius of curvature, κ , is defined as $1/R$. This relates the strain to the radius of curvature, as

shown in Equation 2.9. From the neutral axis the axial stress is defined by Equation 2.10.

$$\epsilon = \frac{y}{R} = \kappa y \quad (2.9)$$

$$\sigma_{ax.} = E\kappa y \quad (2.10)$$

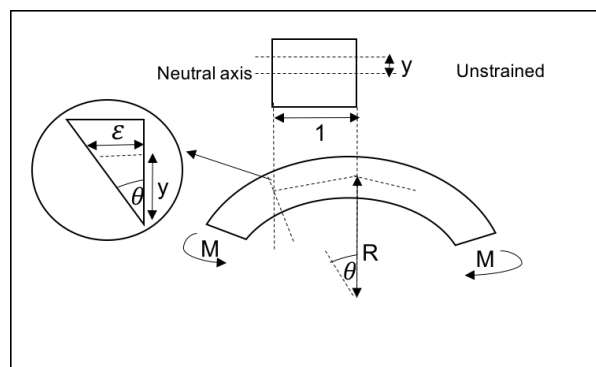


Figure 2.2: Bending moment

By using Equation 2.9 and Equation 2.10, the bending moment can be written as shown in Equation 2.11. The last term of the equation is the moment of inertia, I , which means that the equation for the bending moment is written as shown in Equation 2.12.

$$M = E\kappa \int y^2 dA \quad (2.11)$$

$$M = \kappa EI \quad (2.12)$$

Based on this it is possible to prove that the material properties are good enough to withstand the forces applied to the structure. It is common to include a security factor to the resulting bending stress, to make sure that the component satisfy the requirements for its use. For components used in aerospace applications, a security factor of 1.5 is required, based on military standards [6].

2.2.1 Bending test

An important factor when designing a component, is to test the ability to resist load requirements. Theoretical and practical results do not always correlate perfectly, which means that physical tests are necessary to verify theoretical design calculations. A bending test, done as a four point test, will make it possible to detect if the component fulfill the required strength properties. The presence of two loading points, makes the maximum flexural stress spread between the loading points of the component, i.e. the stress concentration extends over a larger region, compared to a three point test where the load is located to one point. For composites, as non homogeneous materials, this is an advantage to avoid premature failure. When the component is bent, the convex side of the component, might achieve the maximum tensile load. The concave side of the component, might achieve the maximum compressive load. If the maximum tensile or compressive load is reach first, depend both on the material and the construction of the component. However, in most cases the tensile load will be reached before the compression load, which means that the maximum flexural strength often refers to the maximum tensile stress.

Four point bending test is a frequently used engineering test, for mechanical testing of components. Two supporting points are placed at the underside of each end of the part, and their function is to support the part i.e. no load applied. Furthermore, two load points are added in the middle, perpendicular to the longer axis of the component. A sketch of a test setup, according to ASTM C393 and ASTM D7264 [7, 8], is illustrated in Figure 2.3. Increasing the applied load, will bend the structure until it breaks. A crack that occurs along the load direction where the point loads are applied, is what forces the component to break. The test is used to measure the maximum load a component could be exposed to, before it causes critical failure.

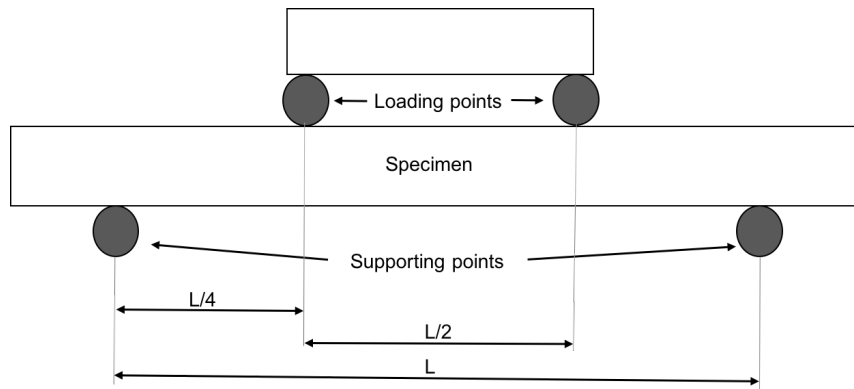


Figure 2.3: Four point bending test

2.3 Buckling analysis

When axial loads are applied to a structure, and transversely deformations occur, increase or decrease of stiffness to the structure are possible results. Tension will increase the stiffness, while decrease in stiffness is a result of compression loads. This will change the cross-sectional area, and the change in stiffness will change the eigenfrequencies of the structure [9]. If the structure is subjected to bending, compression loads arise in some parts of the structure. Failure due to buckling might be the result, even at loads lower than the materials ultimate compression strength. This means that material properties, geometry of the instance and support of elements of the cross section, all are factors that affect the possibility of buckling failure [5]. However, material failure and collapse are possible results when deformations are unavoidable, and is important to take into consideration. In this section theory about how linear elastic eigenvalue analysis is performed in Abaqus, is presented.

In Abaqus linear elastic eigenvalue buckling is based on search for where the model stiffness matrix becomes singular [10]. This is when Equation 2.13 has nontrivial solutions.

$$\mathbf{K}^{MN} v^M = 0 \quad (2.13)$$

\mathbf{K}^{MN} is the tangent stiffness matrix, v^M is nontrivial displacement solutions, and the

coefficients M and N refer to degrees of freedom. For structures with an aligned loading, buckling will occur at a bifurcation point. I.e. the intersection point where the primary and secondary equilibrium paths intersect. Every possible mode of buckling has its own bifurcation load, and in an eigenvalue buckling analysis the critical loads are the eigenvalues, λ_i . The first point where the tangent stiffness becomes unstable, is found by splitting the tangent stiffness matrix into the material stiffness matrix, \mathbf{K}_0^{MN} , and the geometric stiffness matrix, \mathbf{K}_Δ^{MN} . \mathbf{K}_0^{MN} depends on the base state and possible preloads, while \mathbf{K}_Δ^{MN} depends on the component forces. Then Equation 2.13 is resolved into Equation 2.14.

$$(\mathbf{K}_0^{MN} - \lambda_i \mathbf{K}_\Delta^{MN}) v^M = 0 \quad (2.14)$$

As a final statement it is worth to mention that a linear elastic analysis often gives excessive results. In most cases nonlinearity and imperfections impede the structure to achieve the theoretical buckling values. To get a more realistic value it might be necessary to perform more complicated analysis, e.g. nonlinear analysis. However, in this master work the analysis is primarily used for control of the design, and a linear elastic analysis will be sufficient.

3. Preliminaries

In this chapter calculations and discussions carried out prior to both the analysis and experimental work are presented. It is important to make sure that the same elements and values are used in both aspects, to make theoretical and practical results comparable. Geometries of models, layup sequences and material properties are included.

3.1 Models and requirements

Two different models of the joiner, are represented with different geometries, hence a rectangular box profile and an I-beam. Figure 3.1 illustrates geometries of the models. The length is set to 598 mm, with height of 56 mm and width of 43 mm. The rectangular box profile is hollow, while the I-beam has a core inserted in the middle of its web. Requirements, given by Kitemill, states that the joiner should resist a load correspondent to 2000 kg. For a component on earth, this correlates to a load of 19620 N. The weight of the joiner should be as light as possible, according to the strength requirements.

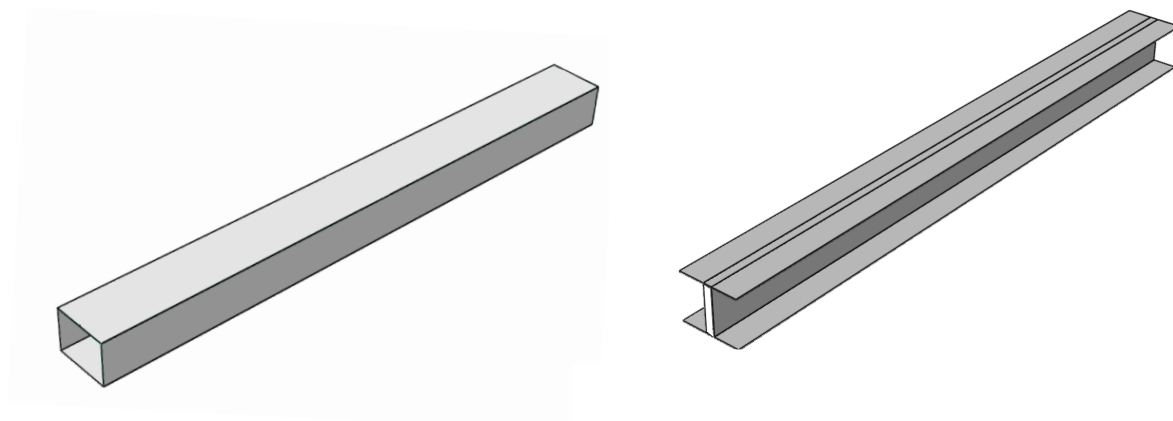


Figure 3.1: Geometries of models

Sharp corners might cause excessively high stresses, which means that rounded corners are preferable [11]. For the I-beam corners who combines web to flanges, should be rounded. For the rectangular box profile corners between sides and top or bottom of the structure, should be rounded.

Calculations of needed thicknesses for the joiner to withstand the applied forces, were carried out during the specialization project [2]. Furthermore, tests done by Kitemill shows that torsion, moment and forces of the sides, are negligible. With a few corrections of material properties, due to more specific data obtained, the needed thicknesses could be calculated. Results corresponding to the values in Table 3.1 were attained. The calculations were performed by a Matlab-program, developed in the specialization project.

Table 3.1: Preliminary thicknesses

Profile	Thickness(sides/web)	Thickness(top/bottom/flange)
Rectangular	5.8 mm	4.7 mm
I-beam	1 mm	3.5 mm

Note that the calculated values are minimum thicknesses for a unidirectional material, to resist the given forces. This means that other factors, e.g. use of woven material or stacking sequence, might affect the values. An additional calculation and explanation related to this issue, is included in Section 3.3.

3.2 Material properties

The material used in the production of joiners, was HexPly 8552 5HS with carbon fibers of the type IM7. This is a woven prepreg, which means that for each ply in the 0° -direction, there will be fibers in the 90° -direction. Correspondingly there will be fibers in both $+45^\circ$ and -45° for plies in the 45° -direction. The core used in the I-beam was of the type Rohacell 110 Rist-HT. This is a foam core made of polymethacrylimide (PMI). Material properties are given in Table 3.2 for Hexply 8552 5HS and in Table 3.3 for the Rohacell core.

Table 3.2: Material properties for HexPly 8552 5HS [12]

Property	
Mass [g/m ²]	374
ρ [g/cm ³]	1.77
E_x [GPa]	86
E_y [GPa]	86
E_z [GPa]	10
ν_{xy}	0.005
ν_{xz}	0.005
ν_{yz}	0.5
G_{xy} [GPa]	5.0
G_{xz} [GPa]	2.84
G_{yz} [GPa]	2.84
X_T [MPa]	850
Y_T [MPa]	850
X_C [MPa]	900
Y_C [MPa]	900
S_{xy} [MPa]	70
S_{yz} [MPa]	70
CPT [mm]	0.300 \pm 0.015

Table 3.3: Material properties for Rohacell 110 Rist-HT 0.005 mm [13]

Property	
ρ [g/cm ³]	0.11
E [GPa]	0.18
ν	0.25
G [GPa]	0.07

3.3 Layup sequence

The strength and properties of the finished joiner are largely determined through the layup sequence, as explained in Section 2.1. Before start of any analysis or experimental work, it is important to do calculations. By using the Matlab-program for thickness calculations as a starting point, developed during the specialization project [2], layup sequence for both joiner geometries are obtained. These calculations include mechanical loading, i.e. bending- and critical buckling stress, and uses this to calculate the thickness the joiner needs to avoid failure. Furthermore, some rules for determining the number of plies in different orientations are needed. Due to interlaminar stresses no more than four consecutively layers in the same direction should be present [14]. Mid-plane symmetry is also important to take into consideration, to avoid deformation e.g. warping. With thickness calculations and these two rules in mind, it is possible to generate a layup sequence for each part.

The material used is HexPly 8552 5HS, with properties as stated in Table 3.2. Estimated ply thickness is set to 0.3 mm. Plies in the 0° -direction maximize the bending stiffness, and plies in the $\pm 45^\circ$ -direction are added to eliminate the tendency for buckling and torsion. The force is primarily in the radial direction, which means that it is preferable with a few more plies in the 0° -direction. Amount of plies in each direction is decided to make the sides, top and bottom of each structure correspondent. I.e. the layup sequence of the sides must consist of the same directions as the end of the layup sequence for the top and bottom, to make it possible to fold the end of the ply and use it as the first or last ply of the next part. This will be further explained during the experimental work in Section 4.1. The calculated values are given in Table 3.4. Note that these values are for the woven fabric, i.e one ply in the 45° -direction account for a ply in both $+45^\circ$ - and -45° -directions. The values stated in Table 3.1, are based on a unidirectional material, however the used material was a woven fabric. The differences in thickness from the values calculated in Table 3.1, are done to make the thicknesses divisible with the layup sequence. These calculations resulted in the laminate stacking sequence, as shown in Table 3.5. Another note to add is that the Rohacell core is not included in this calculations. It is

used to further stabilize the structure, meaning that the carbon fiber skin part should be strong enough to resist applied forces without core included.

Table 3.4: Layup calculations

	Rectangular Top/Bottom	Rectangular Sides	I-beam Flange	I-beam Web
Thickness	5.4 mm	3.0 mm	3.6 mm	1.8 mm
Amount of plies	18	10	12	6
Amount of plies in 0°-direction	10	6	8	4
Amount of plies in 45°-direction	8	4	4	2

Note: Thickness of web represent the thickness of each side of the core.

Table 3.5: Calculated layup sequences

Part	Sequence
Rectangular sides	$[0_2/45/0/45]_s$
Rectangular top/bottom	$[0_3/45_2/0_2/45_2]_s$
I-beam web	$[0/45/0]_s$
I-beam flange	$[0/45/0_2/45/0]_s$

3.4 Theoretical laminate properties

From material properties and layup sequence, together with laminate theory, laminate properties are obtained. By using Equation 2.2, to define the in plane stiffness matrix, the tensile modulus for each laminate is obtained through Equation 2.5. Then, by multiplying the moment of inertia of each structure, the bending stiffness was found. Calculations were done by creating a Matlab-code, which is included in Appendix B. The results are shown in Table 3.6. These values will be used as reference values, when the produced joiners are to be tested. The theoretical values represent a perfect structure, which means that deviations indicate voids in the structure of the produced joiners.

Table 3.6: Theoretical laminate properties

	Rectangular	I-beam
E_x side/web	66.97 GPa	70.65 GPa
E_x top/bottom/flange	64.37 GPa	70.65 GPa
EI	14.97 kN m ²	12.06 kN m ²

Theoretical weight of the joiners could be calculated from the mass of the prepreg, given in Table 3.2. Together with the area of material used, obtained from the layup sequence, width- and length dimensions. For the I-beam the weight of the core were calculated from the density given in Table 3.3, and then added to the weight of the carbon composite skin. The calculated values are given in Table 3.7, and will be compared with the experimental results.

Table 3.7: Theoretical weight

	Rectangular	I-beam
Area of material used	1.80 m ²	1.08 m ²
Weight	672.75 g	417.92 g

3.5 Prototype production

To make it possible to understand how Kitemill works today, and how they are producing their prototypes, a study of their facilities at Lista were performed. Currently, Kitemill is using manual layup as their production method, with fibers and resin separately added into the mold. Curing is carried out in a room holding 40°C. The profile of their prototype is a rectangular box, and the used mold is designed to form the outer dimensions. Furthermore, a rubber balloon is used inside the structure to establish an inside pressure. When the balloon is expanded by air, redundant resin flows out of the structure. Nevertheless, this technique is not fully successful due to burst of the rubber balloon during curing. Polystyrene is used inside the profile to establish higher pressure against the wall, which make the resin flow. After curing, a more compact structure is achieved. However, it is not possible to release the polystyrene from

the joiner when it is fully cured, which means that it is left inside the structure. This is illustrated in Figure 3.2.

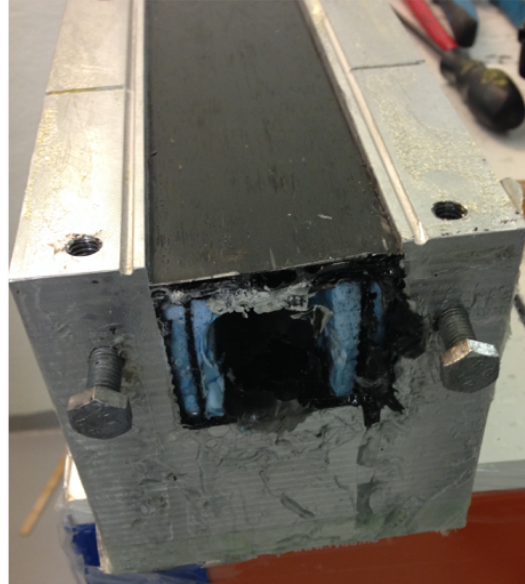


Figure 3.2: Joiner as produced today

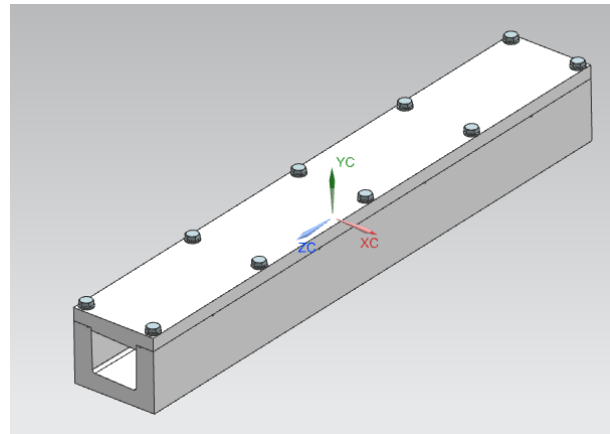
For mass production this method is not preferable, it is slow and time consuming. Furthermore, it is hard to control the end properties of the joiner when fibers and resin are manually added. To ensure the reliability of the joiner, it is important to have control of the process, the quality and end properties, to avoid failure of components in use. This means that a more reliable and efficient manufacturing method should be developed. The challenges with the prototype production, are used as motivation to further develop a more efficient manufacturing method for future mass production.

4. Experimental Work

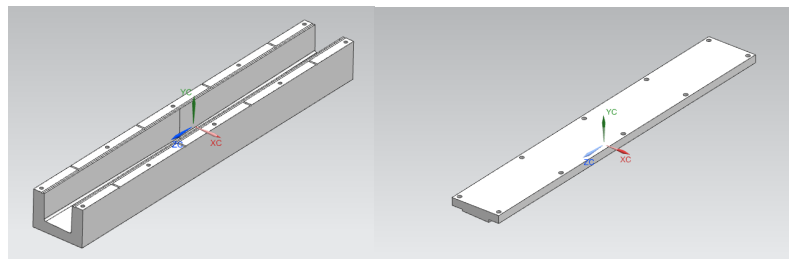
The experimental work consisted of two different structures with the same production processes, i.e. prepreg. After the specialization project [2], it was clear that a further study and comparison of the two structures were necessary to conclude with the most preferable one for the joiner. This chapter consist of a description of how the experimental work was performed.

4.1 Molds

The first step in the experimental studies, is to make a mold for the joiner to be formed, to give the wanted geometric dimensions. A mold that could be used for both the rectangular box profile and the I-beam is preferable. From the drawings of Kitemill's exsisting mold, a mold base was made, as illustrated in Figure 4.1. The mold is made in a way that makes the outer dimensions controllable, which are the critical requirements for the final parts. This is because the joiner is the innermost part of the wing. Currently, Kitemill is using the mold for manual layup, and it is preferable to further test the mold for production with prepreg. In a longer perspective Kitemill is interested in the prepreg process for a more effective and controllable future production. For the rectangular box profile the mold could be used as it is, together with a filled rectangular aluminium profile inside the structure. Insertion of an aluminium profile, means that there is no need for an inside bag during curing in the autoclave. Furthermore, it would make it possible to add pressure both during layup and to the finished part in the autoclave. With a small modification it will form a mold for the I-beam as well. The modification is to insert two filled rectangular aluminium blocks, on each side of the mold, to make the shape of an I-beam. The machine drawings for the top and bottom of the mold, together with the rectangular blocks, are to be found in Appendix A.



(a) Complete mold



(b) Bottom part of mold

(c) Top part of mold

Figure 4.1: Mold base

For both profiles, a technique to combine the sides, top and bottom of the rectangular box profile, and the flanges to the web of the I-beam, was developed. The technique folds plies from the bottom part through the sides, and further up to the top of the mold. That is, the plies of the sides are the same as half of those used in the bottom part, and the first of the plies in the top part of the model. This will then make the part as a whole, without any assembly lines that could make the part weaker. The technique is further described for the rectangular box profile in Figure 4.2 and for the I-beam in Figure 4.3. Furthermore, this means that the layup sequence developed in Section 3.3, must consist of the same plies for sides and web as in the end and beginning of the top, bottom and flanges.

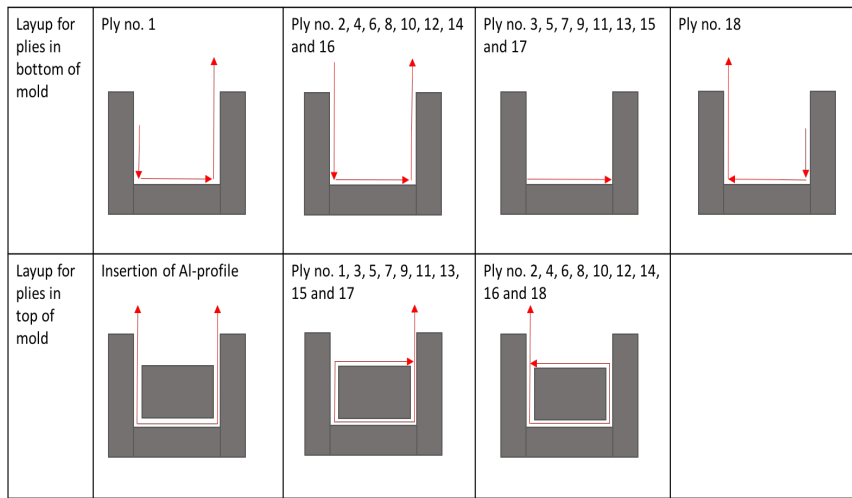


Figure 4.2: Technique used for layup of the rectangular box profile

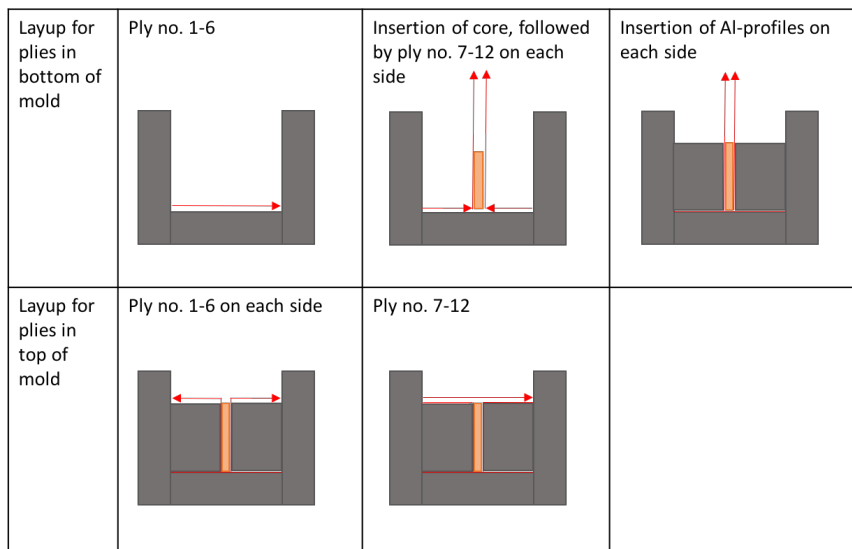


Figure 4.3: Technique used for layup of the I-beam

Before the mold could be used it was released with a release agent. The used release agents were Frekote 44-NC and Frekote 700-NC. A release agent is intended to make the finished part easily removed form the mold after curing. Furthermore, it will give a smoother surface and, if present, seal small pores inside the mold.

4.2 Layup

Layup of both parts were done in the same mold, first the rectangular box profile and then the I-beam. Experience developed during the layup of the rectangular box profile was used to improve the layup of the I-beam. This made the process of the I-beam faster, especially during the demold of the part. Performance of layup for the two different parts, are described in the next sections.

4.2.1 Rectangular box profile

The first ply of the layup was bonded to one of the sides through the bottom and the other side of the mold. The rest of the ply was left open, without being bonded to the structure, as illustrated in Figure 4.4. To make the ply stick better to the mold surface, and to make it lay properly into all edges and corners, a debulk with vacuum pumps was performed.

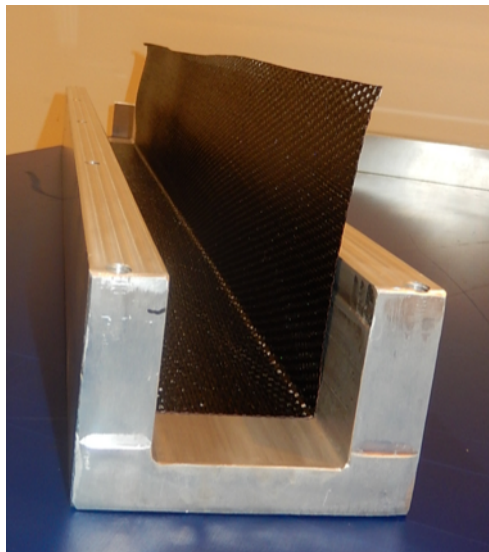


Figure 4.4: Step 1 layup of first ply of the rectangular box profile

The process continued with a sequence of a wider ply followed by a narrower ply. For the wider plies enough material to make a top layer, was left without bonding to the structure. The narrower plies were only bonded to the bottom of the tool. After every second ply a debulk was

performed, and a release film was placed between each of the sides of the wider plies. This was to prevent the layers to stick together during the debulk processes. Figure 4.5 shows both these steps of the layup.

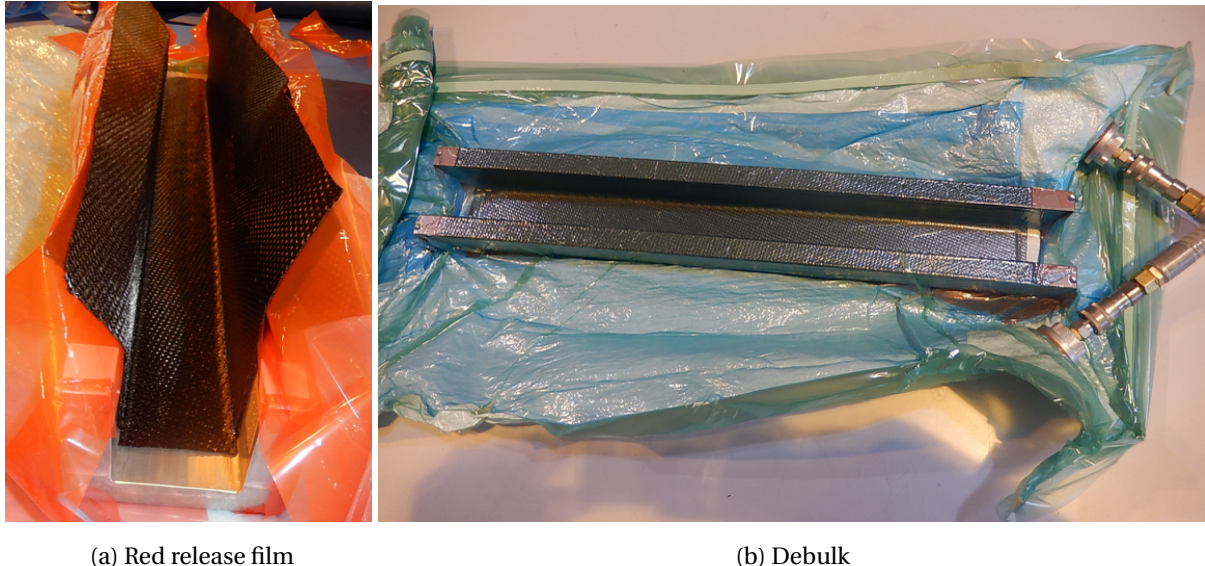
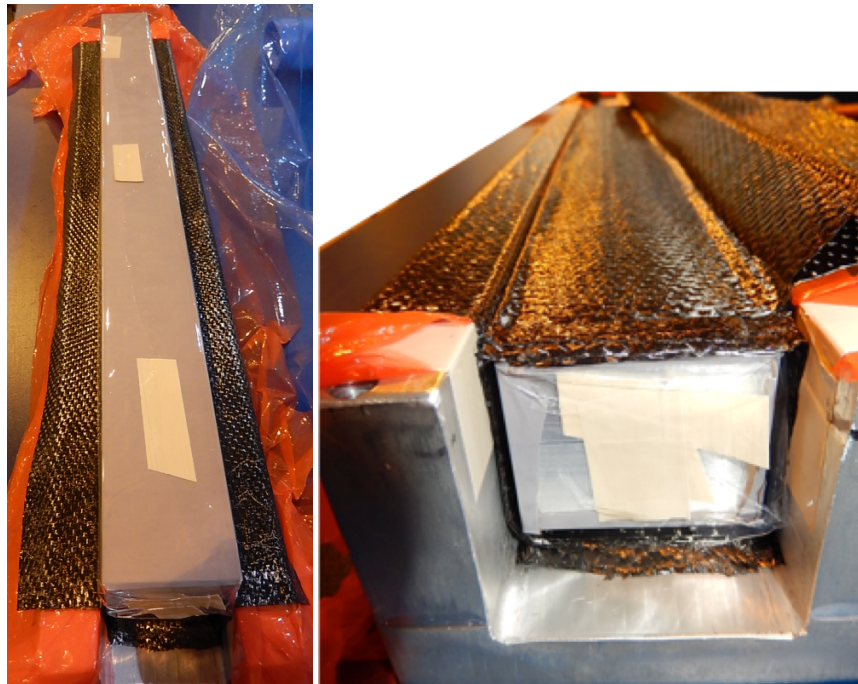


Figure 4.5: Step 2 of layup for the rectangular box profile

When all the 18 plies of the bottom were applied, the technique described in Section 4.1 was used for the layup of the top of the part. To achieve enough pressure inside the structure, and to have something to push the top layers against, the rectangular aluminium profile, was inserted. However, before the aluminium profile was inserted, Frekote 700 NC was applied as a release agent, together with Tooltec, to prevent the part to completely adhere to the inserted mold after curing. This is illustrated in Figure 4.6a. The inset was done before the top plies were laid down, which is shown in Figure 4.6b.

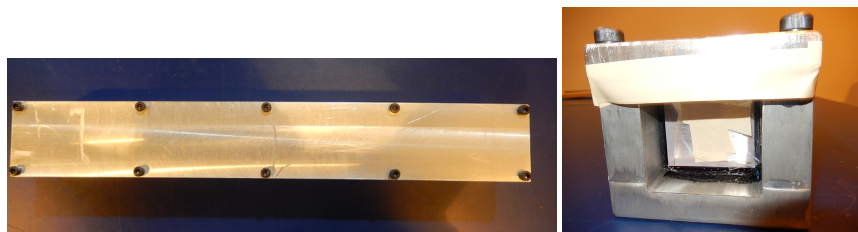


(a) Al-profile with Tooltec

(b) Layup of the top plies

Figure 4.6: Step 3 of layup for the rectangular box profile

After all the top plies were laid down and the whole part was debulked, the top of the mold was inserted and fastened with bolts, as shown in Figure 4.7.



(a) Top view

(b) Side view

Figure 4.7: Top of mold inserted

Then the whole mold was bagged for curing in the autoclave, as shown in Figure 4.8. An envelope bag was used, this means that two of the sides of the bag were already bonded, i.e. only two sides in need for sealing tape. At this step it is important that the bag is able to hold vacuum, and to make sure that this was the case, the pressure inside the bag was checked over

ten minutes. No difference in pressure, means that there is no leak in the bag. Furthermore, to avoid burst of the bag during curing in the autoclave, breather was wrapped around the whole mold. Some extra breather was put at both ends of the mold, to make sure that when vacuum is present, it does not force the bag to move into the gap between the mold and the part. In that case, burst of the bag is reasonable. Figure 4.8a shows the mold with breather before the vacuum is coupled on. With vacuum coupled on, the part was ready for the autoclave, as shown in Figure 4.8b. The used cure cycle consisted of 650 minutes with a temperature range and dwell at 180 °C for 375 minutes.



(a) Before vacuum applied

(b) Ready for autoclave

Figure 4.8: Bagging of the rectangular box profile

4.2.2 I-beam

For the I-beam the mold base together with two filled blocks of aluminium, inserted inside the mold base, were used. The first six plies of the I-beam were bonded to the bottom of the mold, and debulk performed for every second ply, as shown in Figure 4.9.

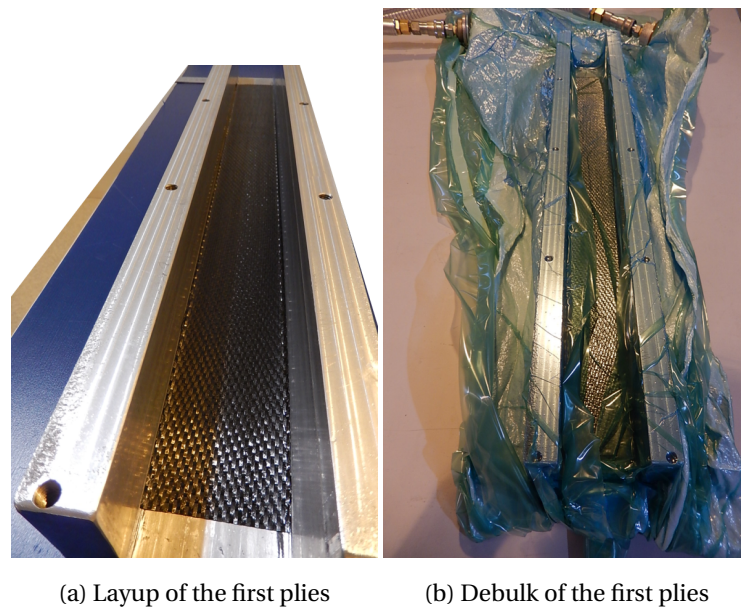


Figure 4.9: Step 1 of layup for the I-beam

After the first six plies, the 5 mm Rohacell 110 Rist-HT core was inserted, together with two side plies. The side plies were bonded to the bottom of the structure, but the ends were open, until all the six side plies were applied. Moreover, before the core was inserted, it was dried at 120 °C for one hour. To avoid moisture inside the part, which could cause failure inside the structure, it is important that the core is completely dry. After all the side plies were applied to the bottom of the part and to the core at the sides, two aluminium profiles were inserted, as described in Section 4.1. Release film was added between each ply, to avoid them to stick together during the layup. Then the rest of the side plies were bonded over the aluminium profiles, which made them form an outward C, as illustrated in Figure 4.10. After the insertion of the aluminium profiles and the layup of plies surrounding them, some space between the core and the top of the C-shaped plies occurred. This could cause air inside the structure, which then could cause failure and is not preferable. To account for the possible failure, a few thin layers of fibers were inserted.

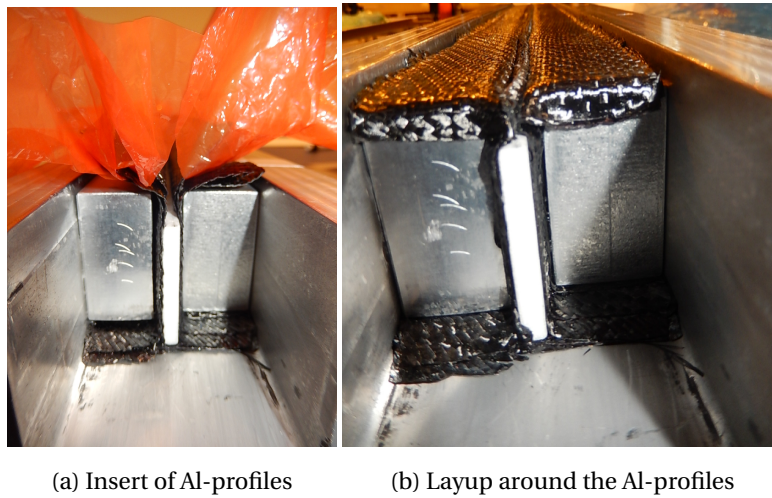


Figure 4.10: Step 2 of layup for the I-beam

The layup ended with another six plies bonded to the top of the mold, and they were bonded to the rest of the structure by inserting the top to the mold, and then fastened through bolts. This is shown in Figure 4.11.

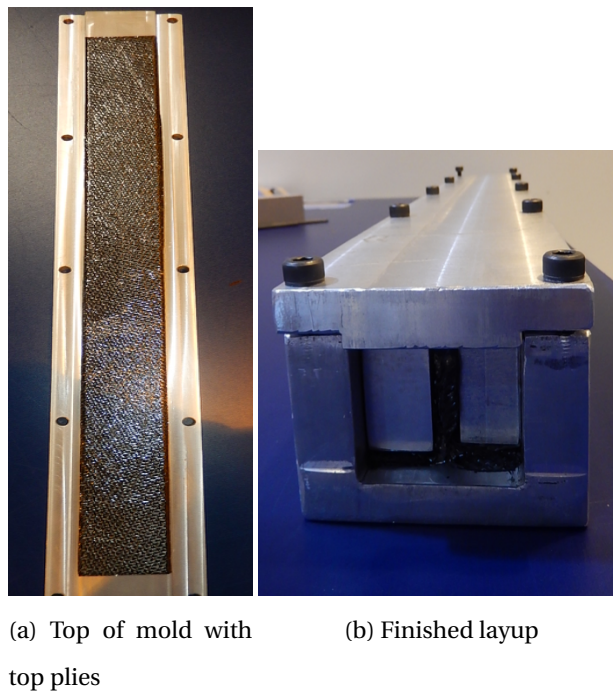


Figure 4.11: Step 3 of layup for the I-beam

The same bagging procedure as for the rectangular box profile was followed, with an envelope bag and sealant tape around the open edges. The part was wrapped in breather, and the finished bagged part ended up as shown in Figure 4.12. Pressure inside the bag was checked over ten minutes, no difference in pressure was obtained and the bag was considered leak free.



Figure 4.12: Bagging of I-beam

To make sure the same curing conditions were representative for both profiles, the used cure cycle was the same as for the rectangular box profile. This cycle had a total time of 650 minutes and a dwell at 180 °C for 375 minutes.

4.3 Demolding

The finished cured parts came out of the autoclave, without any bag brushing and turned out as shown in Figure 4.13.



Figure 4.13: Demold, after autoclave

For the I-beam a pressure tool was used to release the part from the mold. The inner aluminium profiles were easily removed with some blow of a hammer. The rectangular box profile was harder to demold, the main reason was the use of a different release agent than used for the I-beam. On the rectangular box profile Frekote 44 NC was used as the release agent, due to difficulties under the demolding, it was decided to use Frekote 700 NC for the I-beam. This release agent made the part release easier from the mold, and is therefore the preferred one. Furthermore, it was harder to remove the inner aluminium profile of the rectangular box, due to locked walls at all sides, this will be further discussed in Section 6.3. However, after a good amount of hard blows from a hammer, the aluminum profile released, and the joiner turned out fine.

4.4 Results

The joiners were polished to achieve a smooth surface, and the finished parts are shown in Figure 4.14.

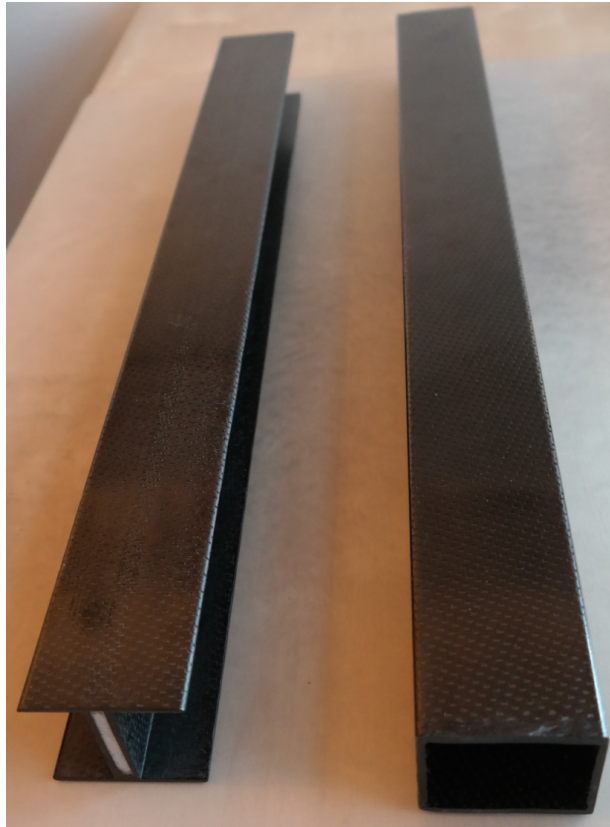


Figure 4.14: Finished joiners

The parts were measured to control weight, length and thickness dimensions and the results are stated in tables 4.1 - 4.3. These values are the average of four measurements at different points of the respective region.

Table 4.1: Measured length and weight of the produced parts

	Rectangular	I-beam
Weight	729 g	472 g
Length	598 mm	598 mm

The theoretical weights of the joiners were stated in Table 3.7. Compared to these values the obtained weights from the experimental work, have some deviations. Both joiners were heavier than the theoretical values indicate. This might be due to that the theoretical values are based on mass per area for an uncured ply, given in the material data. Some deviations from this mass might exist, and could be the explanation to the higher results.

Table 4.2: Measured thicknesses of the produced parts, top and bottom

	Flange of I-beam	Rectangular box
Top		
Side 1	2.39 mm	3.92 mm
Side 2	2.32 mm	3.93 mm
Bottom		
Side 1	2.53 mm	4.34 mm
Side 2	2.53 mm	4.32 mm

Note: Side 1 and side 2 represents the two different ends of the part.

Table 4.3: Measured thicknesses of the produced parts, sides

	Web of I-beam	Rectangular box
Side 1		
Core	4.59 mm	-
1	2.61 mm	3.14 mm
2	2.45 mm	3.07 mm
Side 2		
Core	4.85 mm	-
1	2.47 mm	3.04 mm
2	2.52 mm	3.08 mm

Note: Side 1 and side 2 represents the two different ends of the part. On each side there is two walls, which are represented as 1 and 2.

Compared to the values calculated in Section 3.3, and stated in Table 3.4, some of the measured values corresponds well, while others deviate more from the theoretical values. The values differ the most at the top of the rectangular box profile and at the top flange of the I-beam. This might be due to complications with some plies to fully cover the whole length, after being bonded to both sides and the bottom of the mold. The explanation to the lower thickness might then be a result of some fewer plies over a gap from each side of the top part. To avoid this problem in a future production, it is recommended to estimate more material than needed at each end, and then use a knife or scissor to cut it of later. However, after some cycles of debulking, the prepreg is stiffer and might be hard to cut. When it comes to the sides of the web of the I-beam, it is worth to note that these dimensions were hard to measure correctly. The core in the middle made it hard to fasten the micrometer. This will be further discussed in Section 6.1.

4.5 Testing of components

The produced joiners were tested through a four point bending test, and followed requirements from ASTM C393 and ASTM D7264 [7, 8]. The tests were performed in the Fatigue Lab at IPM NTNU. Schematic view of the test setup is shown in Figure 4.15.

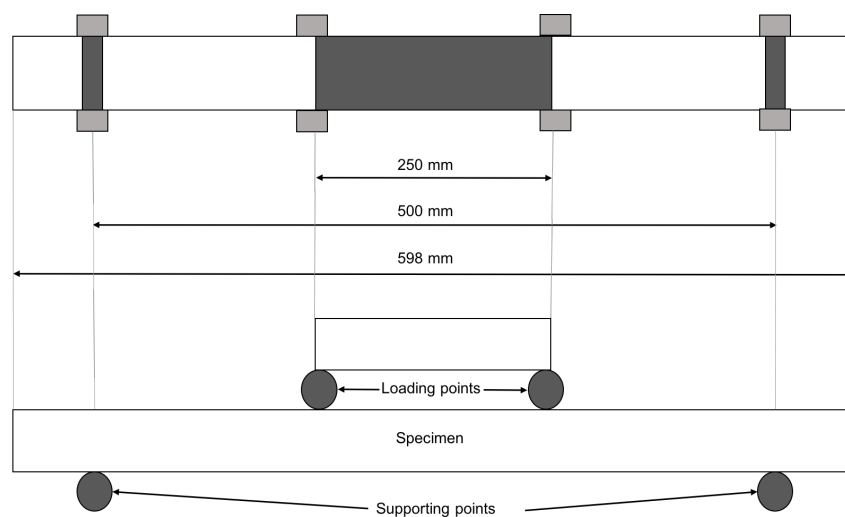


Figure 4.15: Schematic view of test setup

For the bending test a test machine with a load capacity of 250 kN was used, the experimental setup is shown in Figure 4.16. The machine was controlled by an Instron controller. Before the joiners were placed inside the test machine, strain gauges were placed at three different points, two in the axial direction, at the top and bottom of the structure. The third was placed at one of the sides, in the 45° -direction, to ensure that no displacement occurred in this direction. The load span had a length of 250 mm, with each load point placed 174 mm from its adjacent end. The support span had a length of 500 mm and the supporting points were placed 49 mm from its adjacent end.



Figure 4.16: Test setup for four point bending test at IPM NTNU

The test speed was, at first, set to 0.1 mm/min to insure that the test setup was correct, later the speed was increased to 1 mm/min. Added load was gradually increased and displacement data detected. When maximum load capacity was reached, the load was reduced. Displacement data was obtained while the load gradually decreased against zero.

4.5.1 Results

The bending test resulted in fracture of both joiners. For the rectangular box profile the fracture started under one of the loading points, the fracture was gradually developed after the maximum load was reached. Figure 4.17 shows the resulting rectangular box profile after the four point bending test. The I-beam also achieved some fracture where the loading points were placed. Furthermore, there were some bending of the flanges. The I-beam with fracture, after the four point bending test, is shown in Figure 4.18.

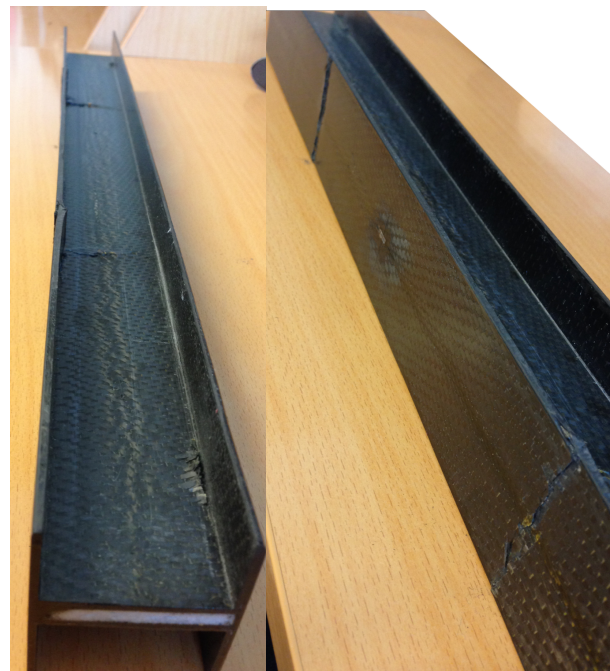


(a) Over all



(b) Most fractured area, under loading point

Figure 4.17: Results after four point bending test for the rectangular box profile



(a) Over all

(b) Fracture on the upper side

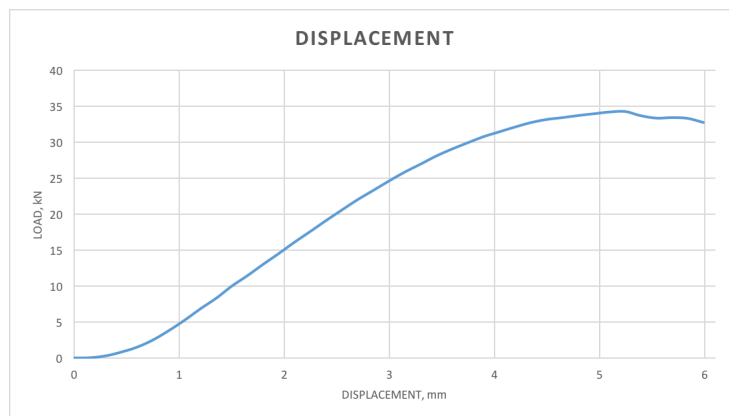


(c) Fracture under loading point

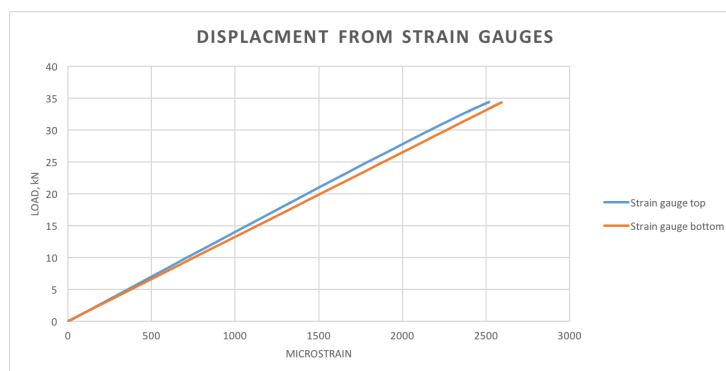
Figure 4.18: Results after four point bending test for the I-beam profile

For the rectangular box profile the maximum load capacity was reached at 34.33 kN, and for the I-beam at 36.01 kN. The displacement curves are shown in Figure 4.19a and Figure 4.20a, for the rectangular box profile and I-beam respectively. Both displacement curves show a slow start, where both displacement and load are approximately zero. The reason might be that the whole test setup need some time to establish a stable position. When this is achieved, stable relationship between load and displacement is accomplished. Furthermore, it should be noted that the values of the displacement on the displacement curve from the Instron controller, does not represent the displacement of the joiner. It represents the total displacement on the whole

system, including e.g. fixture, which means that these values should not be used to determine the maximum displacement of the joiners. The rectangular box profile has a consistent displacement curve, while the curve of the I-beam shows some inconsistency at the very end. This could be due to construction, i.e. the closed structure of the rectangular box profile, makes the whole structure bend. For the I-beam, with a more open structure, the bending of the web and flange will be different, which could explain the inconsistency.

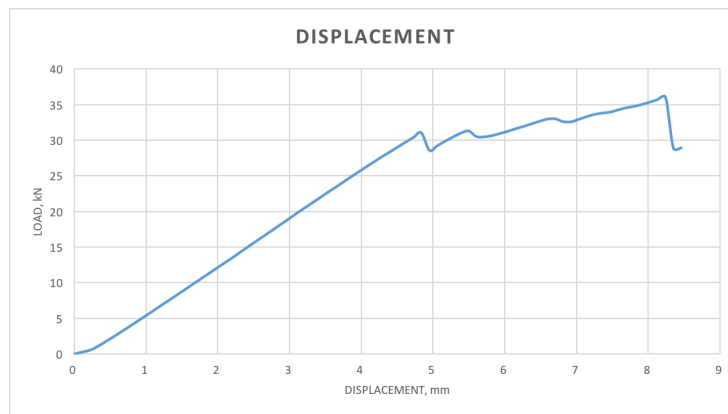


(a) Instron measurements

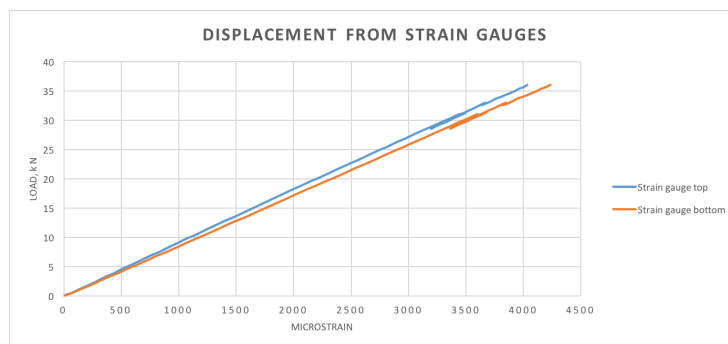


(b) SG measurements axial direction

Figure 4.19: Displacement curves for rectangular box profile



(a) Instron measurements



(b) SG measurements axial direction

Figure 4.20: Displacement curves for I-beam

Maximum strain for the rectangular box profile was 0.002592, and 0.004224 for the I-beam, as shown in Figure 4.19b and Figure 4.20b. The strain gauge placed at the top of the structure, will be subjected to compression. While the strain gauge placed at the bottom of the structure will be subjected to tension. Measured strain, from the strain gauges, shows a linear relationship to the applied load, for both structures in tension and compression. It should be noted that the absolute value of tension and compression are used to make them comparable. Right before maximum load is reached, the curve of the I-beam shows a notch. This corresponds to the inconsistency of the displacement curve. The linear strain curve emphasize the brittleness of composite structures, i.e. when the maximum load capacity is reached, fracture occurs.

From the test data, bending stiffness of the structures were calculated, using Equation 2.12, and compared to the theoretical values. Detailed description of the calculations are given in Appendix C. Results are stated in Table 4.4, together with the deviation in percentage. Deviations from the theoretical values, are further discussed in Section 6.1. However, it is clear that the bending stiffness of the rectangular box profile was higher than that of the I-beam. Compared to the difference in layup sequence and thickness of each laminate, the results correspond well. Furthermore, this shows that even if the thicknesses of the I-beam laminates were smaller than for the rectangular box profile, it resisted a higher load. This will be further discussed in Section 6.2.

Table 4.4: Comparison of tensile modulus

	Rectangular	I-beam
Theoretical	$EI = 14.97 \text{ kNm}^2$	$EI = 12.06 \text{ kNm}^2$
Test result	$EI = 17.75 \text{ kNm}^2$	$EI = 11.45 \text{ kNm}^2$
Deviation in percent	18.57%	5.06%

5. FE-Analysis

FE-analysis is a good tool to verify design safety, and is widely used as a method to test new designs in an inexpensive way before production starts. There are a manifold of software packages available at this area, the one used for this work is Abaqus 6.14, form Dassault Systemes. In this chapter a discussion of imperfections and element types are performed, together with description and results form the FEA, bending- and buckling analysis.

5.1 Imperfections

When deciding which model to use, it is important to keep in mind that the best model will be the simplest. It should still be as realistic as possible to compare the simulation results with physical results at a later stage. However, some imperfections will appear.

As a general rule a shell model should be sufficient if the dimensions of the cross-section are less than 1/10 of a typical global structure dimension [15, 16]. This means that for the joiner where the length is over ten times larger than the thickness dimensions, a shell model will be appropriate. Furthermore, by using shell elements the time spent to perform the analysis is shorter. This is due to that fewer elements are needed, compared to a solid based model. Within the shell elements there are two types; conventional- and continuum. Conventional elements represent the model by defining the geometry at a reference surface, and the thickness of the part is defined through the property definition. For continuum elements the entire three dimensional part is represented by volume elements, which means that the thickness of the part is defined from the element nodal geometry [17]. Figure 5.1 illustrates the difference in a schematic way. For most modelling cases, the conventional shell elements predict proper and reliable results and should be used. Hereafter, if not specified, conventional shell elements will be referred to as shell elements.

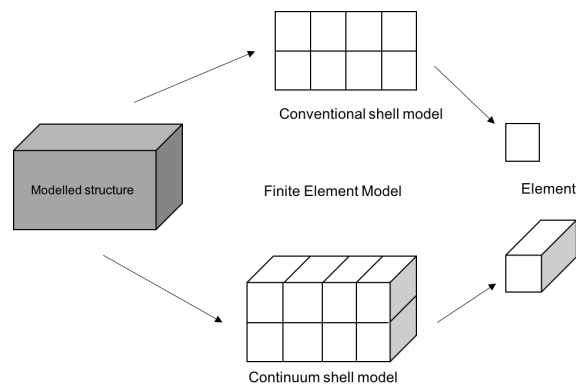


Figure 5.1: Difference between continuum and conventional shell elements

Within the shell element types Abaqus uses several different terms, together with conventional and continuum elements. These include thin, thick and general purpose shell elements [4]. The thin shell elements assume that the transverse shear deformations are zero. All these are conventional shell elements, and are not accurate for composites with thick laminates and small transverse shear modulus. The thick shell elements, on the other hand, do not estimate the shear deformation to be zero. In general, composite materials have low shear modulus, which make it important to include the shear deformation. Last, the general purpose shell elements could be used to simulate thick shell elements [4].

When creating a layup sequence in Abaqus, there are two different possibilities for shell models; conventional- and continuum composite layup. The difference between these two reflects the inequalities between conventional and continuum elements. This means that the conventional model approximate only the reference surface of each ply, while the continuum model represents each of the plies as a whole, but with a kinematic behaviour [18]. However, it is also possible to make a solid composite layup, though this is only preferable for some specific cases, and as long as it is possible a shell layup should be used.

5.2 Model calibration

5.2.1 Geometries

The geometries for the two models are made out of the sketches for the joiner, as shown in Figure 5.2 and Figure 5.3. Both models were made with a length of 598 mm, height of 43 mm and width of 56 mm. For the I-beam the core was set to a thickness of 5 mm and height of 43 mm. The height of the core was set to 43 mm, instead of 35.8 mm, to avoid gap between core and skin in the model. This is a result of that the skin was simulated as a shell model, while the core as a solid. The thickness of the flange of the I-beam will be represented through the section and not the geometry. Meaning that for the modelled structure to have a geometry with a reference surface height of 43 mm, the core needs the same height to avoid a gap between core and skin. The method was chosen to make the geometries of the two joiners the same height, and for better comparison with the experimental model. To establish points for load and support correlative to the bending test, both models were partitioned, as shown in Figure 5.2b and Figure 5.3c, for the rectangular box profile and I-beam respectively.

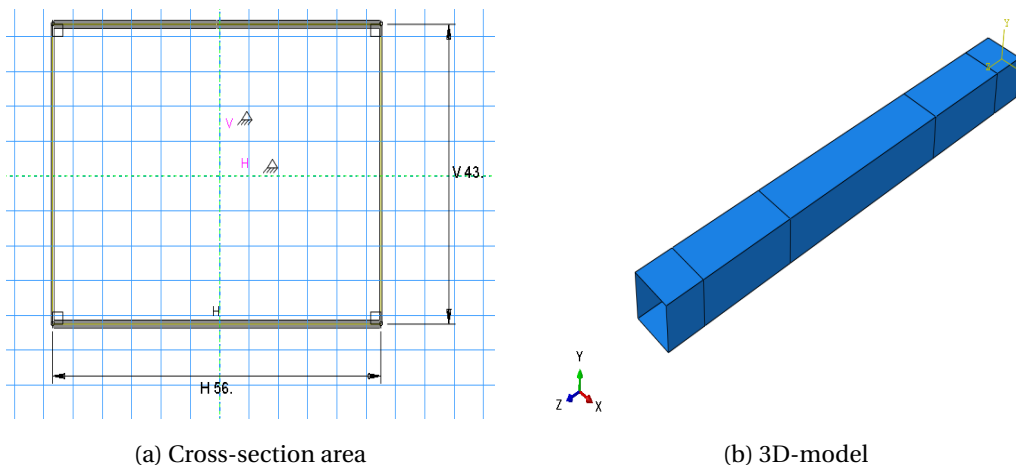
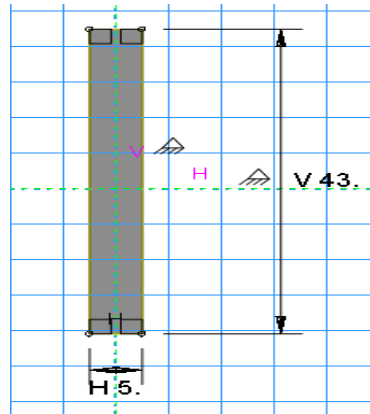
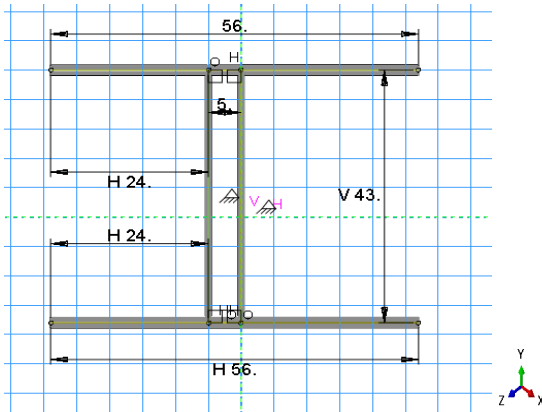


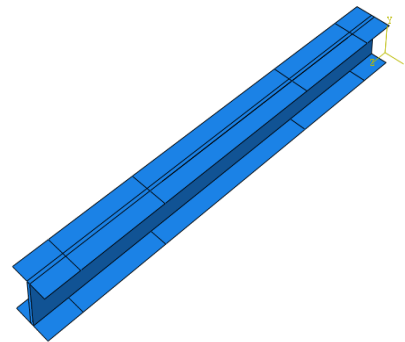
Figure 5.2: Geometry for the rectangular box profile



(a) Cross-section area for core



(b) Cross-section area for skin



(c) 3D-model

Figure 5.3: Geometry for the I-beam

5.2.2 Materials

The materials used in the analysis were assigned to the models by creating sections. The rectangular box profile and the skin of the I-beam were created as shell composites, while the core of the I-beam as a solid homogeneous section. For the used carbon composite, HexPly 8552 5HS, engineering constants were used, and the material properties are stated in Table 5.1. For the Rohacell core the material properties were given as isotropic, and these are shown in Table 5.2. Layup sequences for the composite sections were as stated in Table 3.5. Material orientations were defined as global orientations, with the z-axis as the 1-direction, corresponding to the 0° -direction of the laminate. The transverse direction, the x-axis, was

defined as the 2-direction, and the normal axis in the y-direction.

Table 5.1: Material properties for HexPly 8552 5HS used in the analysis

Property	Carbon/Epoxy composite
ρ [tonne/mm ³]	1.77×10^{-9}
E_1 [MPa]	86 000
E_2 [MPa]	86 000
E_3 [MPa]	10 000
ν_{12}	0.05
ν_{13}	0.05
ν_{23}	0.5
G_{12} [MPa]	5000
G_{13} [MPa]	2840
G_{23} [MPa]	2840
X_T [MPa]	850
Y_T [MPa]	850
X_C [MPa]	900
Y_C [MPa]	900
S_{12} [MPa]	70
CPT [mm]	0.3

Table 5.2: Material properties for Rohacell used in the analysis

Property	Carbon/Epoxy composite
ρ [tonne/mm ³]	1.1×10^{-10}
E [MPa]	180
ν	0.25

5.2.3 Loads and boundary conditions

Boundary conditions were added to impede movement in directions where the test equipment will make movement impossible. At a distance 50 mm from the ends, boundary conditions were added to the nodes. Corresponding to the supporting points of the four point bending test. These nodes were fixed in the y-direction. In one of the ends of the joiner, nodes at the two bottom corners were fixed against translation in the z-direction. Finally, one point in the corner at the end was fixed against translation in the x-direction. Applied boundary conditions, are shown in Figure 5.4. A concentrated force, corresponding to the maximum load obtained during the experimental four point bending test, were added to the middle of the joiner through a reference point. An equation, relating the reference point to the two loading points, was added. This makes load added to the reference point corresponding to load added to the two loading points. This is illustrated in Figure 5.4. For the rectangular box profile the applied load was 34.33 kN, and for the I-beam 36.01 kN, which represents maximum load capacity obtained from the four point bending test.

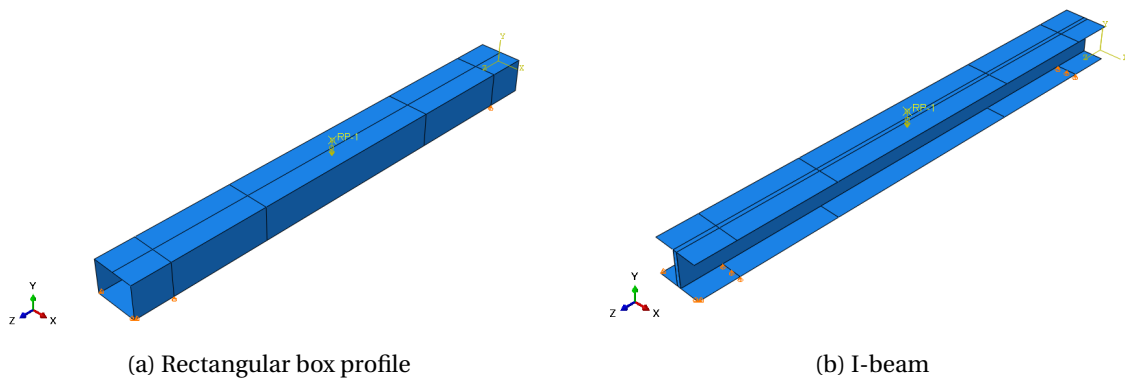


Figure 5.4: Loads and boundary conditions

5.2.4 Mesh

The rectangular box profile, will contain one part i.e. the skin, and it will be sufficient with a shell model. Simulation of the I-beam structure, should be done with two separate parts. The first part consists of the skin of the joiner structure, where the material is carbon fiber composite. For this purpose shell elements will be sufficient. For the second part, consisting of the core, solid elements will be used. The core is used for stabilization, and using a solid core will give a more realistic view of the situation than using a thin shell element, due to allowance of more than one element over the section.

The shell elements, used in the rectangular box profile and for the skin of the I-beam, should be of the type S4R, which is a 4-node quadrilateral stress/displacement shell element, with reduced integration and a large strain-formulation [19], as shown in Figure 5.5a. These elements includes hourglass controls, which makes the model resistant to shear locking. The number of elements used in the skin of the I-beam was 720, and for the rectangular box profile 1220. The geometry of the solid model, i.e. the core of the I-beam, is simple, which allows use of hexahedral or quadratic elements. The simplest of these are the C3D8R, 8-node linear brick elements with reduced integration, which is recommended for simplifications. However, these elements do not have enough integration points, which means that hourglassing could occur if only one element is used thorough the thickness. Furthermore, they are not good to predict bending. By using C3D20R elements, these problems will decrease to an acceptable level. The C3D20R elements are 20-node quadratic brick elements with reduced integration, as illustrated in Figure 5.5b. The number of elements used in the core of the I-beam was 432. Several different sizes of the mesh were tested, which confirmed that changing size did not affect the final analysis result. Details of the meshes for both profiles are shown in Figure 5.6 and Figure 5.7. Total number of nodes for the two models were 1240 and 3395 for the rectangular box profile and the I-beam, respectively. Furthermore, a tie interaction between the core and the skin of the I-beam was added, to make a coupling between the shell and solid elements.

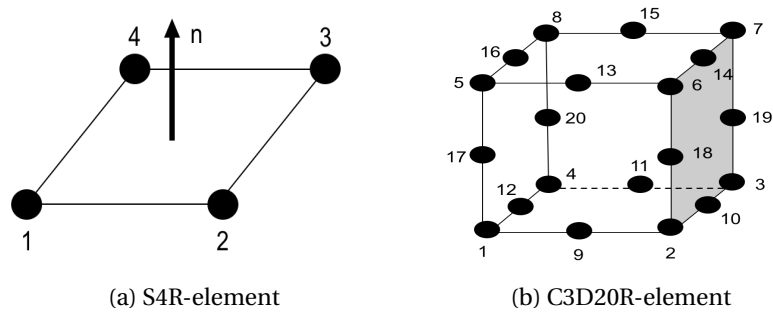


Figure 5.5: Elements used in the analysis

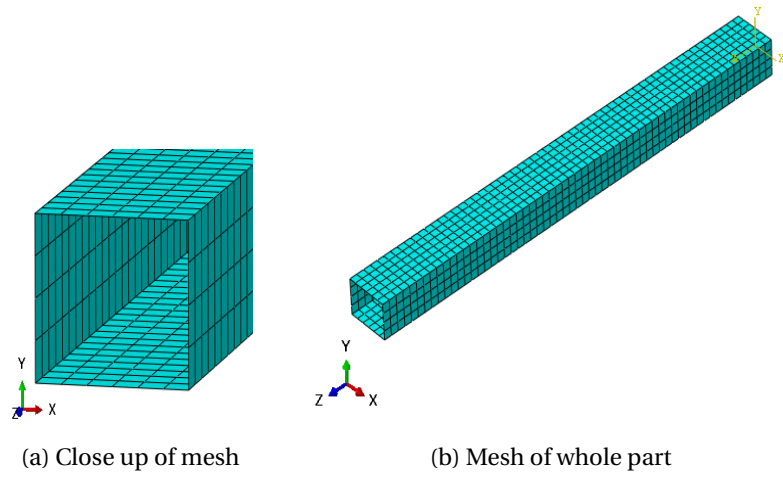


Figure 5.6: Mesh details for rectangular box profile

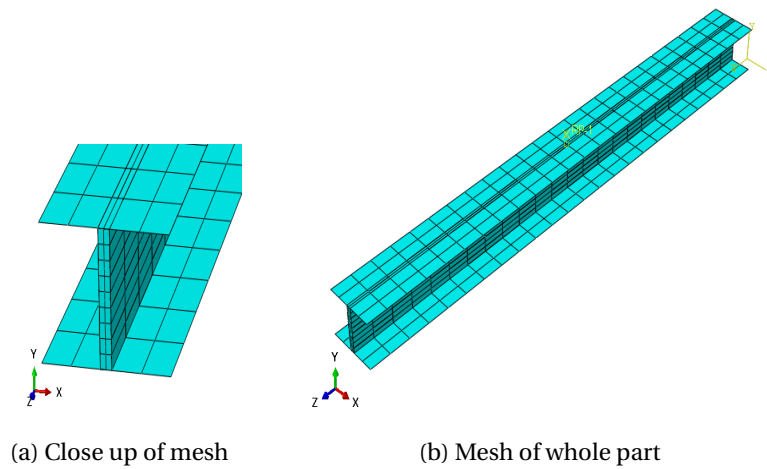


Figure 5.7: Mesh details for I-beam

5.3 Four point bending test

The four point bending test was performed in Abaqus, with the loads and boundary conditions described in the previous sections.

5.3.1 Results

The results from the bending test are shown below, in Figure 5.8 and Figure 5.10, for the rectangular box profile and I-beam respectively. Compared to the results from the four point bending test, the point where the strain gauge was placed, is of interest. This corresponds to the nodes in the middle of the structure. For the rectangular box profile, the results from the analysis gave a strain of 0.002529. This corresponds well with the experimental results, where the measured strain was 0.002592. For the I-beam the analytical result was 0.004459, while the four point bending test resulted in a maximum strain of 0.004224. Furthermore, the load-displacement curves obtained in the simulation have a linear relationship and corresponds well to the curves from the experimental results. These are shown in Figure 5.9 and Figure 5.11, for the rectangular box profile and I-beam respectively. Small deviations from the experimental results indicate that the experimental test performed reasonable results. However, the higher deviation for the I-beam might be a result of a more complex structure to simulate than that of the rectangular box profile. The height of the core of the simulated model was 7.2 mm higher than the experimental model. As seen in Figure 5.10, the area surrounding the core has strain values that differs more than the rest of the skin. It is clear that the core in the middle contributes to these differences. For the rectangular box profile, the strain values are the same over the area. This means that the analytical strain value obtained for the I-beam have more elements of uncertainty related, than the rectangular box profile. It is worth to note that for both profiles, the maximum value of strain obtained through the four point bending test was lower than that of the analytical results, with the same applied load. Which further indicates that there are some elements of uncertainty related to the point where the measurements were taken.

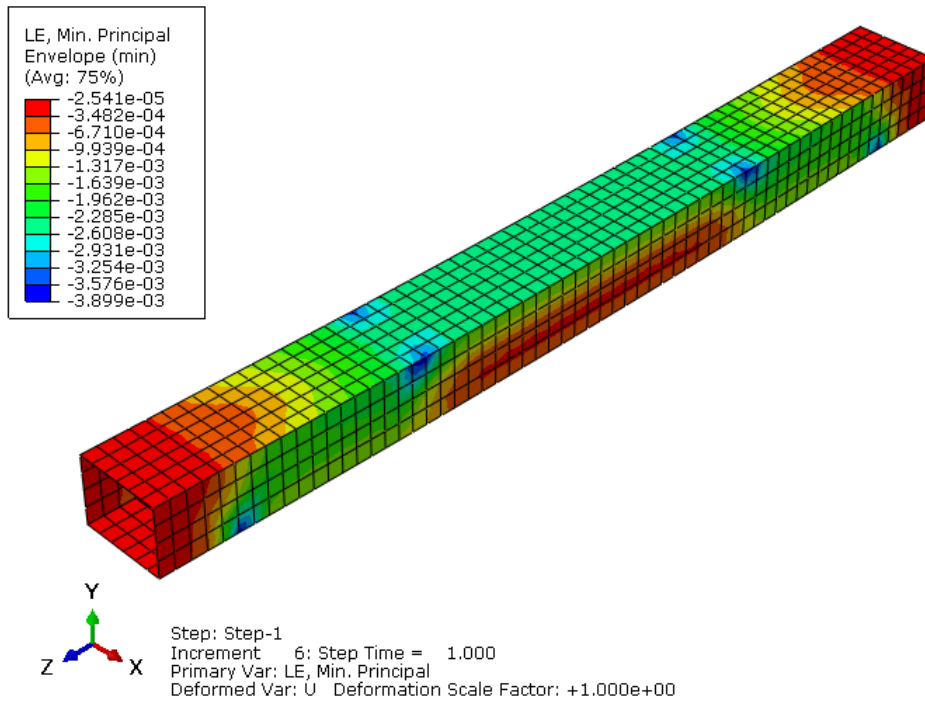


Figure 5.8: Results from four point bending test for rectangular box profile

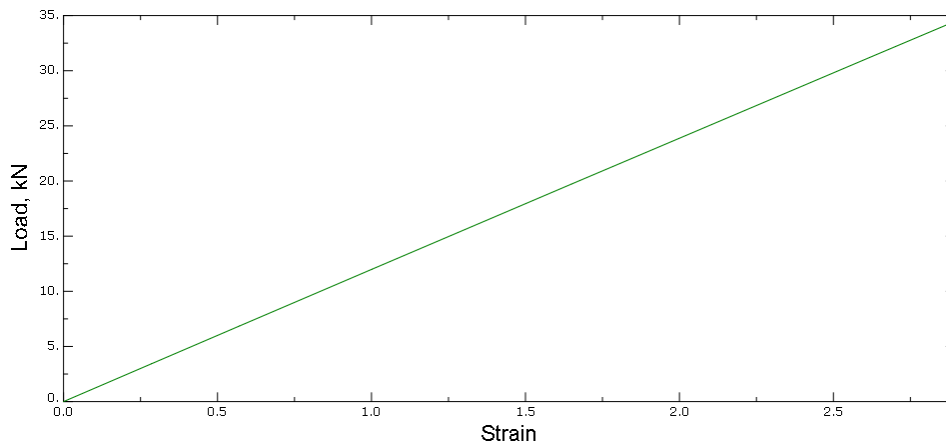


Figure 5.9: Displacement curve of analytical results for rectangular box profile

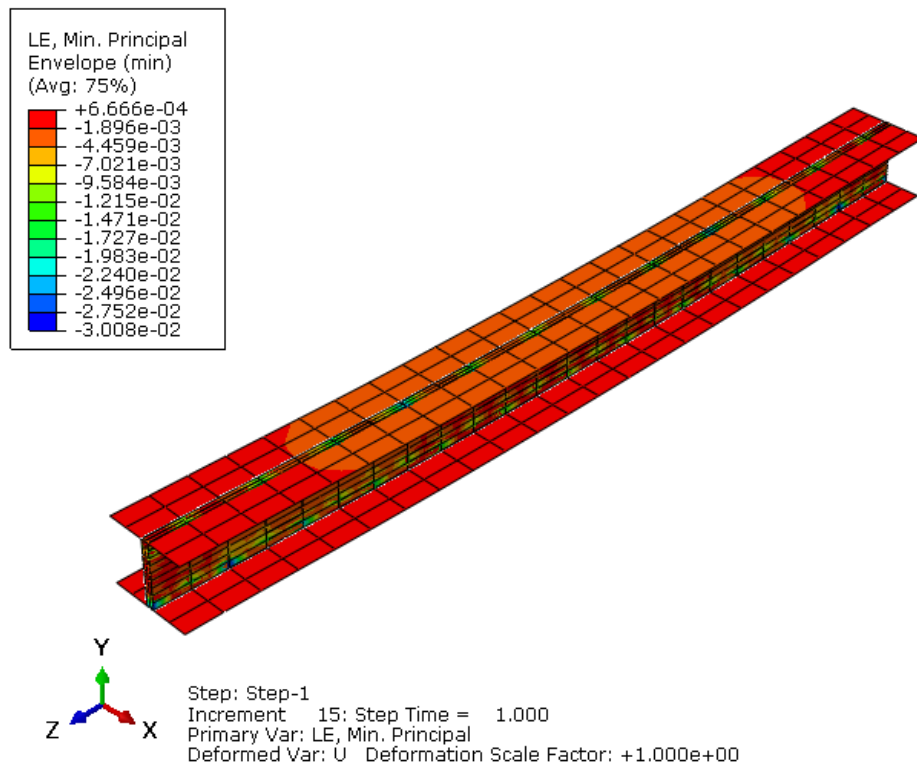


Figure 5.10: Results from four point bending test for I-beam

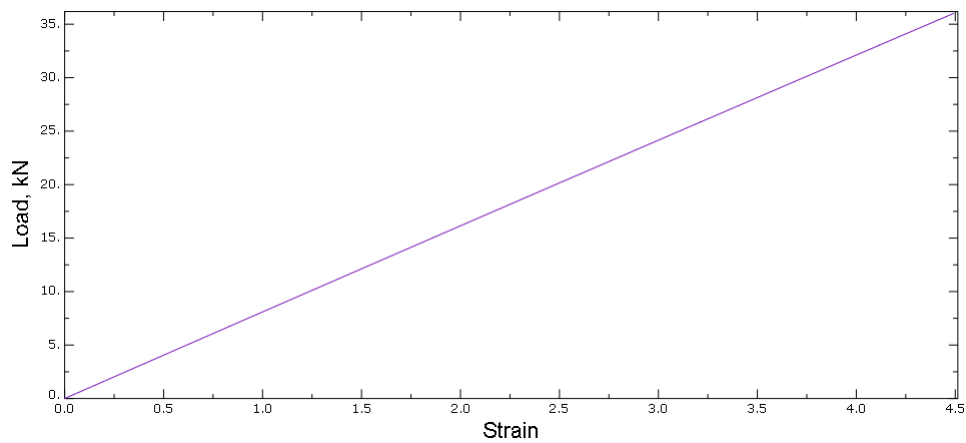


Figure 5.11: Displacement curve of analytical results for I-beam

5.4 Buckling analysis

Critical loads and buckling mode shapes were estimated through a linear buckling analysis. This analysis generates the results by searching for the point where the tangent stiffness matrix becomes abnormal. By using the eigensolver subspace, and the procedure described in Abaqus user manual [10], a linear buckling analysis was performed on both models. Negative eigenvalues indicates that applied load in the opposite direction, will force the component to buckle.

5.4.1 Results

The maximum displacement component is normalized to 1, and indicates that points where this is reached have achieved the critical buckling load. This means that the critical buckling load is used to estimate the buckling deformation of the structure. From a buckling analysis the mode shapes are the most interesting results, due to prediction of the most critical part of the structure. It should be noted that the mode shapes of the loads are only normalized values, which means that the actual critical load are not represented by these magnitudes. However, they indicate differences throughout the structure. To find the buckling load at a specific point, the eigenvalue of the point should be multiplied to the applied load. The results from the analysis are shown in Figure 5.12 for the rectangular box profile and in Figure 5.13 for the I-beam. The buckling load was applied as a point load, using the same equation and reference point as during the analysis of the four point bending test.

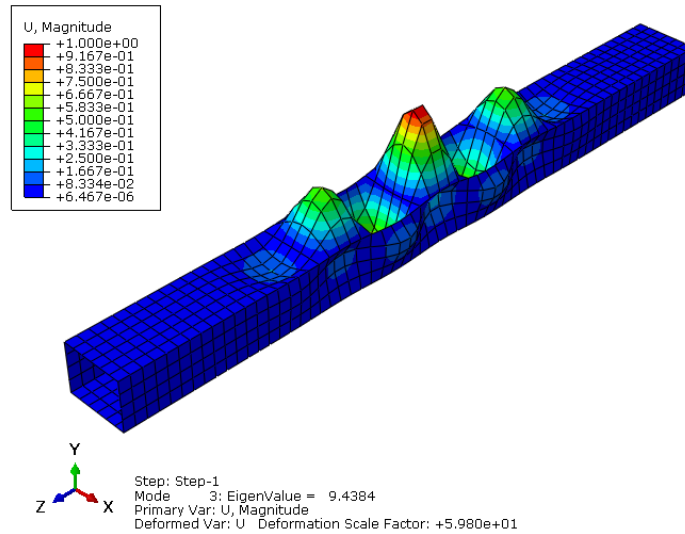


Figure 5.12: Results of buckling analysis for rectangular box profile

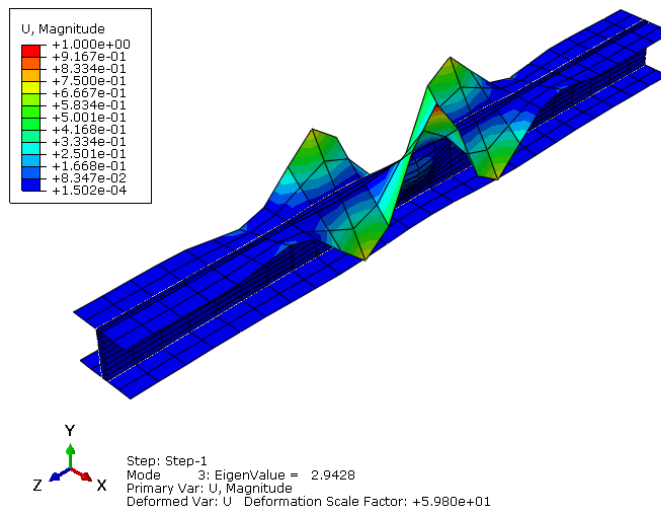


Figure 5.13: Results of buckling analysis for I-beam

Both models show negative values for mode shape 1 and 2, which means that load in the opposite direction would force buckling. For the rectangular box profile the eigenvalue of mode 3 was 9.4384, this should be added to the applied load to reach the buckling load. The corresponding value for the I-beam, was 2.9428. This means that for the rectangular box profile, the critical buckling load is reached at 323.7371 kN, when the maximum load capacity of 34.3 kN is present. Correspondingly for the I-beam at 105.9702 kN, when maximum applied load of 36.01 kN is present. Critical buckling load for the rectangular box profile is higher than for the I-beam, in Section 6.1 this is further discussed.

6. Discussion

During the master work results from experimental and analytical tests, have been evaluated. A discussion where theoretical, analytical and experimental results are further compared should be done to understand the significance of the behaviours. Moreover, a discussion comparing the two different profiles of the joiner is needed, to be able to find the preferred design. At least an evaluation of the manufacturing process and possible improvements should be performed to increase the validation of the developed process.

6.1 Comparison of theoretical and practical results

Theoretical and practical test results, do not always coincide perfectly. There are several possible reasons behind. In the following paragraphs, results from the theoretical calculations, done in sections 3.4 and 3.3, and the analysis, done in sections 5.3.1 and 5.4.1, are further discussed and compared to the results from the experimental work in sections 4.4 and 4.5.1. Calculated and measured values are summarized and compared in Table 6.1.

Table 6.1: Comparison of theoretical and experimental results

	Theoretical				Experimental results				Percent deviation			
	Rectangular		I-beam		Rectangular		I-beam		Rectangular		I-beam	
	Sides	Top/bottom	Web	Flange	Sides	Top/bottom	Web	Flange	Sides	Top/bottom	Web	Flange
Thickness	3.00 mm	5.40 mm	1.80 mm	3.60 mm	3.08 mm	4.13 mm	2.51 mm	2.44 mm	2.66%	23.52%	39.44%	32.2%
Weight	673 g		418 g		729 g		472 g		8.32%		12.92%	
Strain	0.002529		0.004459		0.002592		0.004224		2.49%		5.27%	
Bending stiffness	14.97 kNm ²		12.06 kNm ²		17.75 kNm ²		11.45 kNm ²		18.57%		5.06%	

The most obvious reason behind deviation in experimentally produced parts compared to theory, are the possibility of voids in the structure. During layup of both joiners, there are reasons to believe that the structures have some imperfections. First of all, it was the first time the processes and mold tools were used, which means that the technique for layup had to be

learned as the layup proceeded. That is, the resulting properties of the structures might not be as good as when the manufacturing process is incorporated and mature. This means that for a part to be as perfect as possible, the layup of the part needs to be done more than once. However, small deviations from theoretical results will always exist, making them as small as possible and according to requirements are what makes a produced part certified for use.

For the I-beam there were some problems with debulking the whole part, after the core and the aluminium profiles were inserted, i.e. between the C-layers. This might have caused some air between the layers. However, expansion of the aluminium profiles during heating together with applied vacuum around the whole structure, should restrict the possibility of high air concentrations inside the structure. Another possible imperfection is bridges, that might have occurred in corners and edges. In the beginning of both layup processes this was easily controllable, but the more plies added, harder to control. As far as possible it was kept under control, and the fact that both joiners finished the curing in the autoclave without failure, lower the probability of considerably large amount of bridges in the structure. However, it is worth to mention that the quality of the laminate will increase with a more reliable vacuum pressure control. As already mentioned in Section 4.4, there were some issues with a few of the plies during layup of the top part. This was due to that some of the plies might not have been sufficiently stretched or worked through out the sides. The result was that edges of the top consists a few plies less than the middle of the structure. It should be noted that the angles were measured and plies cut manually. Deviations in angle of fibers, might affect the strength properties of the part, e.g. compression properties. With use of a cutting machine these issues could be ignored, and the uncertainty related to this will decrease. However, the shorter plies resulted in that areas close to the edges consist of some fewer plies than the rest of the top and bottom part of the structure. Nevertheless, the measured thicknesses show higher deviations than what were found in the strain and bending stiffness results. This means that the thickness deviation did not necessarily influence the resulting properties considerably.

Furthermore, it is worth to discuss that only one of each joiner was produced. This means that the results from the experimental test have elements of uncertainty. If more parts of the same profiles are made, and tested at the same conditions, the test results will be more reliable, and as the process is improved, it might be more like the theoretical results. However, it is also worth to mention the fact that crack growth started where the load cell and loading points were placed. Fracture marks give distinct impression of that the deformation is a result of directly contact with the load cell. This means that placement of a piece of a tender material between the load cell and the joiner, might give a higher maximum load. A higher maximum load, will give a higher strain. Assuming the linear strain curve still valid, which means that higher displacement follows a higher load. From equations 2.9 and 2.12, it is clear that increased strain increase the radius of curvature. Furthermore, higher applied load will give a higher bending moment in the structure, as explained in Section 2.2. That is, the joiner might resist higher stresses than the test shows. Total collapse of the structure did not occur, which means that a higher strength of the structure could be reached. However, the measured maximum load achieved during the four point bending test, represent the value where the joiner will be out of order. That is, if the joiner is exposed for a load as high, it should be replaced, to avoid failure. Conditions with that high loads will be out of the normal span of what the joiner is exposed to, and if so, most likely the whole plane will be subjected to extreme conditions, not only the joiner.

Buckling analysis, results in Section 5.4.1, verified that critical buckling load is reached at 323.74 kN for the rectangular box profile and at 105.97 kN for the I-beam. These values show that buckling will not force the joiners to failure before the maximum load capacity is reached. This means that the joiners will be approved for use according to buckling analysis. However, some deviations from the reality of the critical buckling load may exist. These could be explained in a possible nonlinearity and imperfections in the structure. The resulting analytical buckling modes might have been impeded by these imperfections, and could explain the deviations. Nevertheless, the analysis were mainly used as a control of the design, which means that the linear model should be sufficient.

Another laminate property it is important to take into consideration, is the ability of moisture absorption. Structures containing epoxy resins tend to absorb moisture when in service, which could cause degradation of mechanical properties [20]. Several variables influence the degradation, e.g. fiber volume and orientation. The joiner and the kite are exposed to rough weather conditions, e.g. wind and rain. Properties of a laminate could be affected to a considerably level, which means that strength and life of the component might decrease, confirmed by several studies done at the area [21, 22]. Furthermore, the studies found that fiber orientation has influence on moisture absorption, unidirectional laminates have a higher absorption rate than laminates with different orientations. However, failure modes of the laminate were not affected of the moisture absorption. For the joiner this emphasize that different orientations of the plies in the layup sequence are important. Use of a woven fabric makes this easier feasible than use of a unidirectional material, and would therefore be preferable.

In the analysis done in this thesis, the used material properties are those from the material supplier, and do not include properties of wet conditions. Moisture absorption could reduce the compression strength with up to 37%, depending on the layup sequence [22]. How the compression strength of the laminate decrease is important to consider. If it is parts of the laminate that are affected, or the whole structure. Assuming the whole structure affected, the obtained maximum load capacity could be used as an evaluation factor. For the produced joiners, the maximum load capacity obtained through the four point bending test gave the same displacement curves for both joiners, shown in figures 4.19b and 4.20b, for tension and compression. This means that even if the joiners failed due to tension or compression, the obtained maximum load will be the lower, as stated in Section 2.2.1. The joiner is required to resist a load corresponding to 2000 kg, or 19.62 kN. To be able to comply the requirements even if moisture defects are present, a load capacity correspondent to 2740 kg, or 26.88 kN, is required. The maximum load capacity of both joiners, 34.33 kN and 36.01 kN for the rectangular box profile and the I-beam respectively, were above this value. However, testing due to moisture absorption was outside the scope of this master work. It is important to further test the joiner in the conditions of its service, to detect the possible defects over time.

6.2 Profile evaluation

From the measured weights after production of the two different joiners, values given in Table 4.1, the weight of the rectangular box profile was significantly higher than that of the I-beam. This means that according to the requirement of lowest possible weight of the structure, the I-beam is the profile of choice. Furthermore, the lower weight is a result of thinner laminates needed to achieve the same strength. This means that less material was needed to produce the I-beam, than the rectangular box profile. Then it is likely to assume that if the same laminate thicknesses were used, the I-beam would have achieved a significantly higher strength than the rectangular box profile.

The weight of the I-beam is not the only property that counts in its favour. The more open structure, and the fact that the inserted rectangular aluminium profiles were not totally closed inside the structure, made the demolding of the I-beam easier. Moreover, insertion of a core contributed to further stabilization, during layup of the web plies on each side. With the core in the middle there was something to lay the plies against, which made it easier to achieve enough pressure to the wall, to decrease the possibility of weaknesses, e.g. air, inside the structure. Production of a rectangular box profile with core could be tested to increase the scope of the research. Using a core inside the structure instead of an aluminium profile, makes the demolding of the rectangular box profile easier. Then there is no need to remove inside profiles at all. However, the results from the already produced joiners, shows that the rectangular box profile was almost double in weight compared to the I-beam. This fact, and that the core firstly was used as stabilization and not for strengthening of the joiner, indicates that an I-beam with core would be more preferable than a rectangular box profile with core. I.e. if the only difference from the produced joiners is a core inside the rectangular box profile, it is likely to assume that the I-beam still would be preferable.

Furthermore, it is worth to note that the result of the practical analysis was based on one produced part. As mentioned in Section 6.1, there are some elements of uncertainty connected with it. However, even though the test results might not be perfect, it is possible to compare the manufacturing processes and profiles against each other. This is due to that the same conditions are present for both.

The results from the buckling analysis, in Section 5.4.1, provides a higher critical buckling load for the rectangular box profile. This means that the rectangular box profile will buckle at a later stage than the I-beam. However, both profiles showed a critical buckling load higher than the maximum applied load, which means that fracture due to buckling will not arise before the joiner is out of use. That is, the higher critical buckling result is not in itself an argument that makes the rectangular box profile more preferred than the I-beam. The most important result obtained in the buckling analysis, is however that both structures have an acceptable value of critical buckling load. Compared to the maximum load capacity achieved during the four point bending test.

6.3 Improvement of manufacturing process

Developing a good mold tool is one of the most important steps in a composite manufacturing process. The right tool will give high quality of production. Furthermore, it will make the process more efficient and cost effective [23]. Optimization of the used mold will further improve the manufacturing process. In this section some difficulties with the used mold, and possible solutions are presented.

During the processes some difficulties were observed. Firstly, both were time consuming, and opportunities to make them more efficient should be discussed. Time consuming processes means that the profiles will be too complex for future mass production, and are not intended to be an effective way of producing any parts. The more time spent on a part, the higher the cost, and for small parts of the system, as the joiner is, this high expense is unnecessary.

Use of a different mold, means that the mold used in today's production must be changed. Then it is important to keep in mind that the outer dimensions are the ones that are in need for correctness and smooth surfaces. The main reason for the difficulties during layup, was the design and complexity of the mold. A possible improvement is to divide the mold into different parts, which could be easily bonded together during layup and divided during demolding. However, as experienced through demolding, use of the right release agent is highly important, to make the demolding as effective as possible. For this propose Frekote 700 NC turned out to be a better release agent than Frekote 44 NC. With use of the right release agent together with further experience in demolding the part, the process will be faster and more reliable. The more a process is used and incorporated, the faster it would be. Nevertheless, this does not mean that the process is perfect as it is, and that there is no need for further research to make the manufacturing more efficient. The proposed first step to establish a more efficient manufacturing process, is to divide the existing mold into separate parts. This adjustment will make use of the existing equipment, which means that there is no huge change in the process.

Demolding of the rectangular box profile was harder than that of the I-beam. First of all this was related to the inserted aluminium profiles. The more open structure of the I-beam made the profiles easily removable after the exterior of the joiner was demolded. Locked walls at all sides made the demolding more complicated for the rectangular box profile. Use of a separable mold tool will change the demolding of the outer mold, while the demolding of the inner profiles will remain the same. An inside bag or a rubber balloon could be used to avoid the inner aluminium profiles. The small inside dimensions of the joiner makes it likely to assume that this will be complicated and not contribute to a more efficient process. The prototype production, done together with Kitemill, as described in Section 3.5, emphasize the statement. Furthermore, for both profiles the use of inner aluminium profiles made the layup easier, there was something to press the plies against. Use of an inner bag or rubber balloon will not give the same stabilization.

Several others, [11, 24, 25], have produced I-beams as separate parts, i.e. flanges and web, and then bonded them together. This method could be further developed for the rectangular box profile as well, with all sides produced separately. However, for the joiner this manufacturing method might be complicated, due to the specific requirements of the outer dimensions. Furthermore, structures that are not completely bonded together and contain assembly lines, might be weaker. This indicates that an extra amount of plies must be added to account for the lower strength. A heavier part will be the result, due to more use of material. Use of more material to achieve the same strength, makes this manufacturing method less preferential.

Separately produced web and flange, together with a transition fillet, all assembled together by using an outer skin, is another production method used in other studies [26]. With this method, the connection between web and flange is improved, compared to the method mentioned above. Nevertheless, for use in the joiner, outer dimensions must still be controllable. For the rectangular box profile, this means that each wall could be produced as a separate part, and then assembly lines strengthened by inside transition fillets, connected through a skin. However, insertion of transition fillets and a skin inside the structure, might give some installation problems, due to the small dimensions.

As seen in the manufacturing processes mentioned above, the open structure of the I-beam makes the possibilities for improvement of manufacturing process higher. The rectangular box profile is hard to produce effectively, and more testing is needed to come up with a new method. With that said, both manufacturing methods used worked, and resulted in suitable joiners. However, some improvements to the mold used in this master work, should be done to make the process faster. By dividing the mold into separate parts, that are easily connected and fastened through bolts, both the progress of the layup and demolding might be faster. Furthermore, it will increase the quality and reliability of the components, due to removal of elements of uncertainty related to the process.

7. Conclusion

From the production and testing done in this master work it is clear that the I-beam is preferable for future mass production, rather than the rectangular box profile. The conclusion is based on an easier manufacturing process, lighter weight and higher resistance to fracture. However, further improvements should be done to the manufacturing process before it could be used for mass production.

The results from the four point bending test corresponds well with the FEA analysis, which means that the obtained results are reliable. Furthermore, it shows that prepreg production makes the properties easily controllable, and intended for mass production. Then it is possible to secure that all components hold the requirements, i.e. the quality of the produced joiners are higher. Performed buckling analysis confirmed that critical buckling load is kept at an acceptable level, which means that failure due to buckling will be avoidable for the applied forces.

8. Further Work

Some improvements to the manufacturing process, together with more testing of parts are recommended. The following suggestions are intended for future work. Improvement of today's mold could be done by dividing it into separate parts, which could be bolted together when the layup is finished and loosened during demolding. This should be tested for a more efficient layup- and demolding process. Furthermore, to improve the manufacturing process, more joiners should be produced. To ensure that the properties obtained during the tests in this work are reliable, more test results should be established. This includes more testing around buckling, and an experimental buckling test should be done. Analytical results should not have too high deviations compared to a component in use. Investigations related to moisture, due to wet environments of the joiner should be done. Decrease of material properties should be kept at an acceptable level, and according to the strength requirements. At last supplementary studies related to the cost for the whole process should be done.

Bibliography

- [1] Kitemill's homepage. <http://www.kitemill.no>, Last checked: 12.45, 5. May 2016.
- [2] S. Moen. Composite Wing Kite for Energy Generation. Specialization Project, NTNU, December 2015.
- [3] N. P. Vedvik. Essential Mechanics of Composites. 2014 - R01, p. 15-21.
- [4] E. J. Barbero. *Finite Element Analysis of Composite Materials Using Abaqus*. CRC Press, 2013, p. 96-97, 101-104.
- [5] E. J. Barbero. *Introduction to Composite Materials Design*. Taylor & Francis Group, 1. edition, 1999, p. 138-139, 144-146, 231-239.
- [6] Department of Defense Military Standard. *Military Specification MIL-STD-8856B*. Department of Defense United States of America, October 1990, p. 13-14.
- [7] ASTM International. *C393/C393M-11 Standard Test Method for Core Shear Properties of Sandwich Constructions by Beam Flexure*, November 2011.
- [8] ASTM International. *D7264/D7264M-15 Standard Test Method for Flexural Properties of Polymer Matrix Composite Materials*. ASTM International, April 2011.
- [9] J. Jia. *Essentials of Applied Dynamic Analysis*. Springer, 2014, p. 87.
- [10] D. S. Simulia. *Abaqus/CAE Analysis User's Guide, Version 6.14, 6.2.3 Eigenvalue Buckling Prediction*.
- [11] M.D. Gilchrist, A.J. Kinloch, E.L. Matthews, and S.O. Osiyemi. Mechanical Performance of Carbon-Fibre- and Glass-Fibre-Reinforced Epoxy I-Beams: I. Mechanical Behaviour. *Composites Science and Technology*, 56(1):37 – 53, 1996.
- [12] Hexcel. HexPly 8552 Product Data. Technical report, Hexcel Composites, 2013.
- [13] Evonik Industries AG Performance Polymers. Rohacell RIST Product Information. Technical report, Evonik Industries, 2011.

- [14] D. Gay and S. V. Hoa. *Composite Materials Design and Applications*. CRC Press, 2. edition, 2007, p. 76-77.
- [15] E. J. Barbero. *Finite Element Analysis of Composite Materials*. CRC Press, 2008, p. 61.
- [16] A. J. Sadowski and J. M. Rotter. Solid or Shell Finite Elements to Model Thick Cylindrical Tubes and Shells Under Global Bending. *International Journal of Mechanical Sciences*, 74:143 – 153, 2013.
- [17] D. S. Simulia. *Abaqus/CAE Analysis User's Guide, Version 6.14, 29.6 Shell Elements*.
- [18] D. S. Simulia. *Abaqus/CAE User's Guide, Version 6.14, 12.14 Creating and Editing Composite Layups*.
- [19] D. S. Simulia. *Abaqus/CAE Analysis User's Guide, Version 6.14, 27.1.1 Element Library: Overview*.
- [20] G Sala. Composite Degradation due to Fluid Absorption. *Composites Part B: Engineering*, 31(5):357 – 373, 2000.
- [21] A. B. Zai, M. K. Park, H. S. Choi, H. Mehboob, and R. Ali. Effect of Moisture Absorption on Damping and Dynamic Stiffness of Carbon Fiber/Epoxy Composites. *Journal of Mechanical Science and Technology*, 23(11):2998–3004, 2009.
- [22] A.Revathi, M. S. Murugan, S. Srihari, N. Jagannathan, and C. M. Manjynatha. Effect of Hot-Wet Conditioning on the Mechanical and Thermal Properties of IM7/8552 Carbon Fiber Composite. *Indian Journal of Advances in Chemical Science*, 2:84–88, 2014.
- [23] F. C. Campbell. *Manufacturing Processes for Advanced Composites*. Elsevier Science, 2004, Chapter 4.
- [24] G. Zhou and J. Hood. Design, Manufacture and Evaluation of Laminated Carbon/Epoxy I-Beams in Bending. *Composites Part A: Applied Science and Manufacturing*, 37(3):506 – 517, 2006.

- [25] K.D. Potter, R. Davies, M. Barrett, A. Godbehere, L. Bateup, M. Wisnom, and A. Mills. Heavily Loaded Bonded Composite Structure: Design, Manufacture and Test of 'I' Beam Specimens. *Composite Structures*, 51(4):389 – 399, 2001.
- [26] F. Kosel G. Visnjic, D. Nozak and T. Kosel. Reducing Shear-Lag in Thin-Walled Composite I-Beam Wing Spars. *Aircraft Engineering and Aerospace Technology*, 86(2):89–98, 2014.

Appendices

A. Machine Drawings for Mold

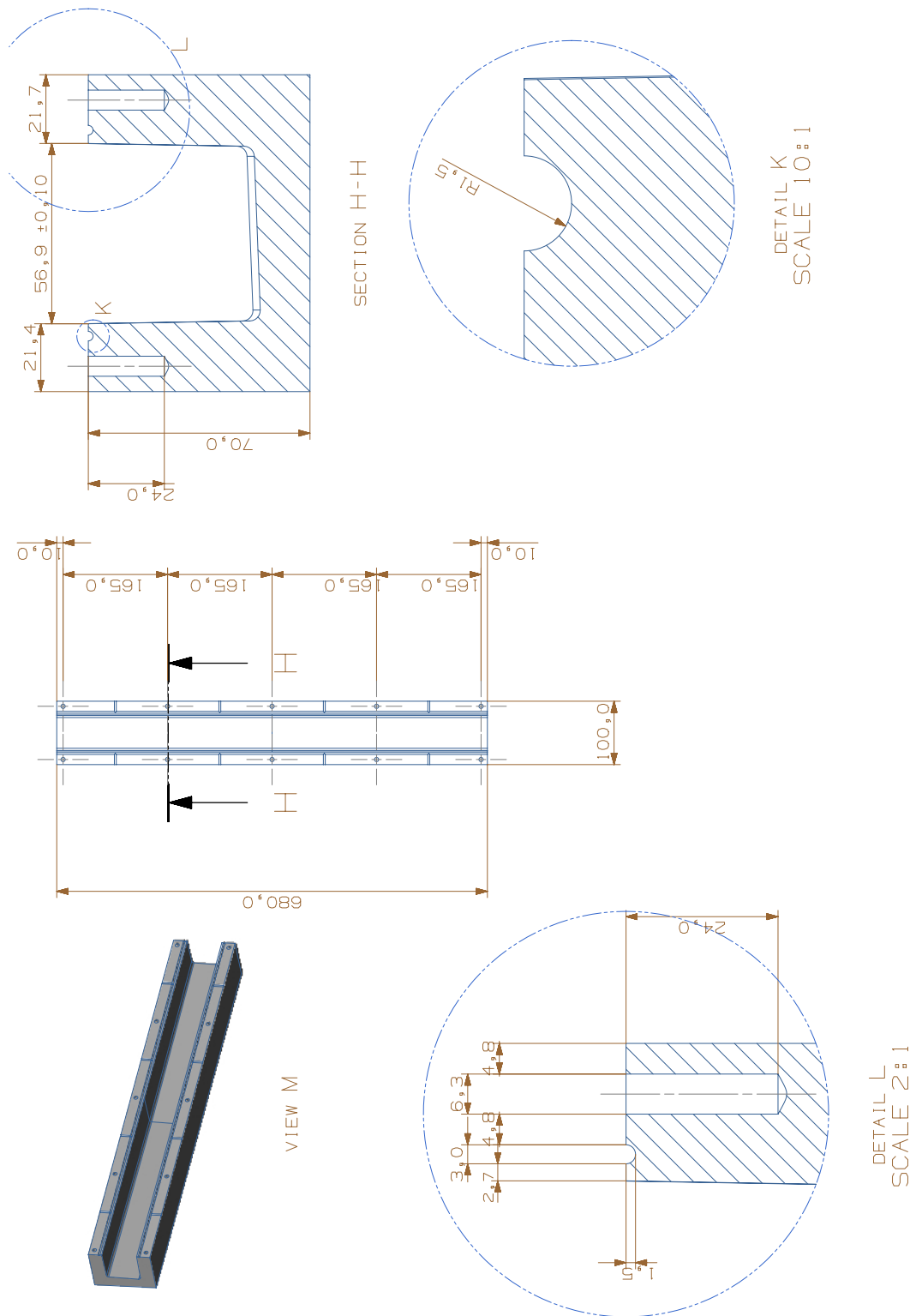


Figure A.1: Bottom of mold

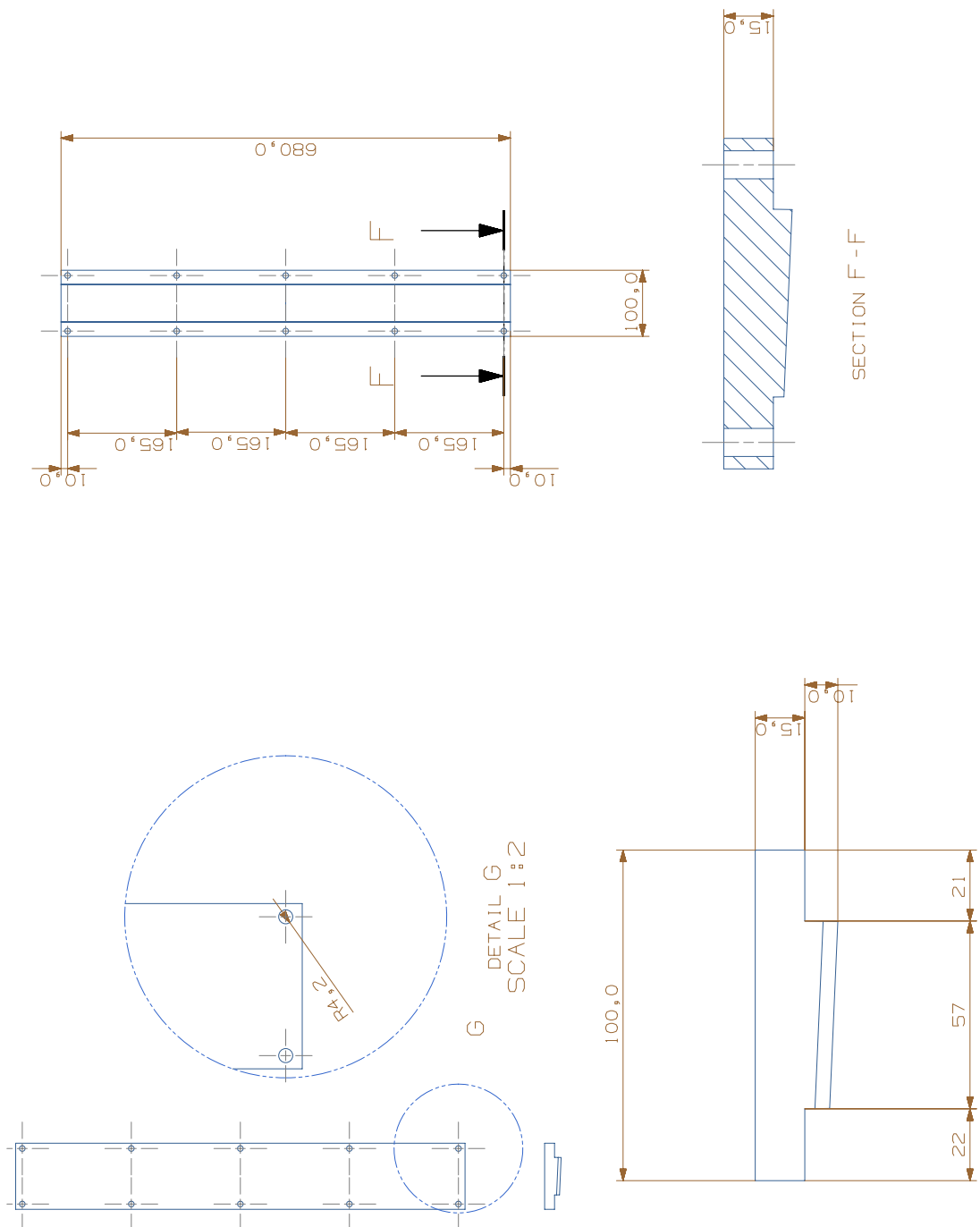


Figure A.2: Top of mold

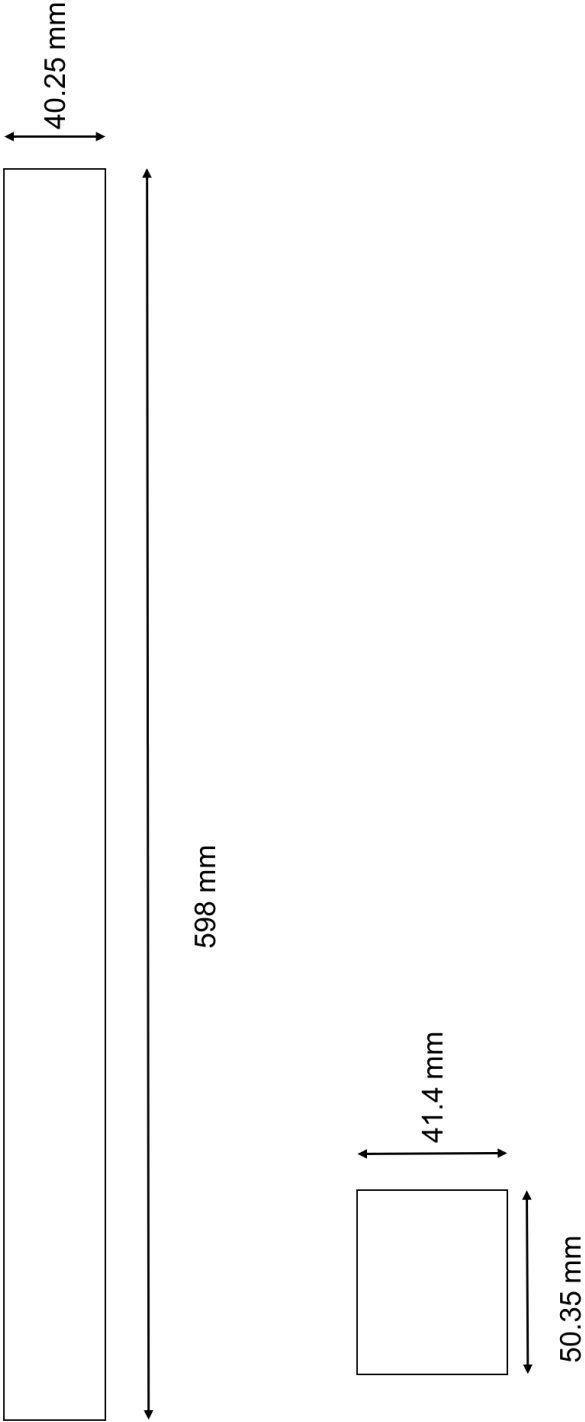


Figure A.3: Inside block for rectangular box profile

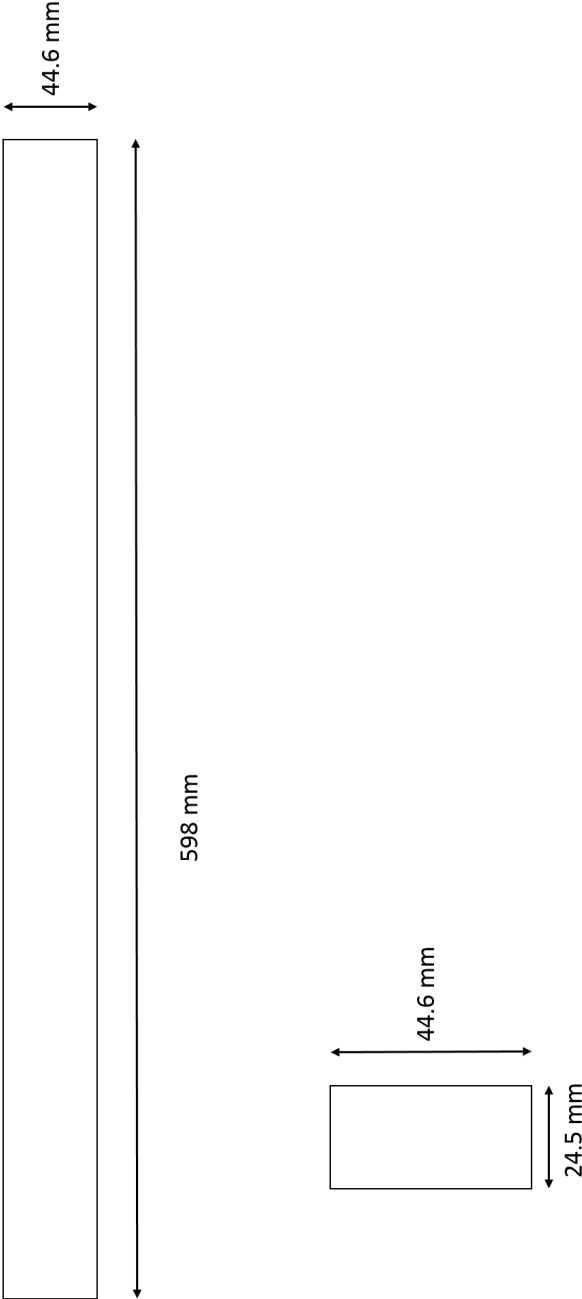


Figure A.4: Inside blocks for I-beam

B. Matlab Code

The following pages describe the Matlab-code used to calculate laminate properties of the joiners. The first code were used to calculate properties of each laminate. Resulting tensile modulus for each laminate where then used to find the bending stiffness for each joiner, through the second code. Note that the error message in the end of the laminate property calculations is only present for the publishing feature, and will not occur if the code runs normally.

```

%Laminate properties calculations

clear all
close all
clc

%Material properties
E1 = 86;
E2 = 86;
v12 = 0.05;
G12 = 5.0;

%Reduced compliance matrix
S = zeros(3,3);
S(1,1)=1/E1;
S(2,1) = -v12/E1;
S(1,2)=S(2,1);
S(2,2)=1/E2;
S(3,3)=1/G12;
S;
C=inv(S);

%Reduced stiffness matrix
Q=zeros(3,3);
Q(1,1)=S(2,2)/(S(1,1)*S(2,2)-S(1,2)^2);
Q(1,2)=-S(1,2)/(S(1,1)*S(2,2)-S(1,2)^2);
Q(2,2)=S(1,1)/(S(1,1)*S(2,2)-S(1,2)^2);
Q(2,1)=Q(1,2);
Q(3,3)=1/S(3,3);
Q;
Sbar=zeros(3,3,3);
Qbar=zeros(3,3,3);

%Layup sequences
Ibeam_web = [0,45,0,0,45,0];
Ibeam_flange = [0,45,0,0,45,0,0,45,0,0,45,0];
rect_sides = [0,0,45,0,45,45,0,45,0,0];
rect_tb = [0,0,0,45,45,0,0,45,45,45,45,0,0,45,45,0,0,0];

layup= input('Which layup do you want to use
(Ibeam_web(1),Ibeam_flange(2),rect_sides(3),rect_tb(4))');

if layup==1
    layup=Ibeam_web;
    r=6;
elseif layup==2
    layup=Ibeam_flange;
    r=12;
elseif layup==3
    layup=rect_sides;

```

```

    r=10;
elseif layup==4
    layup=rect_tb;
    r=18;
end

%Transformation
for k=1:r
    theta(k)=layup(k);
    t(k)=0.3;
    m(k)=cosd(theta(k));
    n(k)=sind(theta(k));

    Sbar(1,1,k) =
    S(1,1)*(m(k)^4)+(2*S(1,2)+S(3,3))*(n(k)^2)*(m(k)^2)+S(2,2)*(n(k)^4);
    Sbar(1,2,k) = (S(1,1)+S(2,2)-
    S(3,3))*(n(k)^2)*(m(k)^2)+S(1,2)*((n(k)^4)+(m(k)^4));
    Sbar(2,1,k) = Sbar(1,2,k);
    Sbar(1,3,k) = (2*S(1,1)-2*S(1,2)-S(3,3))*n(k)*(m(k)^3)-
    (2*S(2,2)-2*S(1,2)-S(3,3))*(n(k)^3)*m(k);
    Sbar(3,1,k) = Sbar(1,3,k);
    Sbar(2,2,k) =
    S(1,1)*(n(k)^4)+(2*S(1,2)+S(3,3))*(n(k)^2)*(m(k)^2)+S(2,2)*(m(k)^4);
    Sbar(2,3,k) = (2*S(1,1)-2*S(1,2)-S(3,3))*(n(k)^3)*m(k)-
    (2*S(2,2)-2*S(1,2)-S(3,3))*n(k)*(m(k)^3);
    Sbar(3,2,k) = Sbar(2,3,k);
    Sbar(3,3,k) = 2*(2*S(1,1)+2*S(2,2)-4*S(1,2)-
    S(3,3))*(n(k)^2)*(m(k)^2)+S(3,3)*((n(k)^4)+(m(k)^4));

    Qbar(1,1,k)
    =Q(1,1)*(m(k)^4)+(2*Q(1,2)+4*Q(3,3))*(n(k)^2)*(m(k)^2)+Q(2,2)*(n(k)^4);
    Qbar(1,2,k) =
    (Q(1,1)+Q(2,2)-4*Q(3,3))*(n(k)^2)*(m(k)^2)+Q(1,2)*((n(k)^4)+(m(k)^4));
    Qbar(2,1,k) = Qbar(1,2,k);
    Qbar(1,3,k) = (Q(1,1)-Q(1,2)-2*Q(3,3))*n(k)*(m(k)^3)+(Q(1,2)-
    Q(2,2)+2*Q(3,3))*(n(k)^3)*m(k);
    Qbar(3,1,k) = Qbar(1,3,k);
    Qbar(2,2,k)
    =Q(1,1)*(n(k)^4)+(2*Q(1,2)+4*Q(3,3))*(n(k)^2)*(m(k)^2)+Q(2,2)*(m(k)^4);
    Qbar(2,3,k) = (Q(1,1)-Q(1,2)-2*Q(3,3))*(n(k)^3)*m(k)+(Q(1,2)-
    Q(2,2)+2*Q(3,3))*n(k)*(m(k)^3);
    Qbar(3,2,k) = Qbar(2,3,k);
    Qbar(3,3,k) =
    (Q(1,1)+Q(2,2)-2*Q(1,2)-2*Q(3,3))*(n(k)^2)*(m(k)^2)+Q(3,3)*((n(k)^4)+(m(k)^4));

end

%Full Laminate Stiffness
T = sum(t,2);
T2 = T/2;
z(1) = T2;
for j = 2:r+1
    z(j) = (T2)-t(j-1);
    T2 = z(j);

```

```

zQbar(:,:,j-1) = Qbar(:,:,j-1)*t(j-1);
z2Qbar(:,:,j-1) = Qbar(:,:,j-1)*(z(j)^2-z(j-1)^2);
z3Qbar(:,:,j-1) = Qbar(:,:,j-1)*(z(j-1)^3-z(j)^3);
end
Qbar;
%ABD Matrix
A = sum(zQbar,3);
a = inv(A);
B = sum(z2Qbar,3)/2;
b = inv(B);
D = sum(z3Qbar,3)/3;
d = inv(D);

%Laminate Material Properties
Ex = 1/(a(1,1)*T)
Ey = 1/(a(2,2)*T);
Ez = Ey;
Gxy = 1/(a(3,3)*T);
Gxz = Gxy;
vxy = -a(1,2)/a(1,1);
vyz = -a(1,2)/a(2,2);
vxz = vxy;
Gyz = Ey/(2*(1+vyz));

%coordinate transformation
theta_u = 20.7;
theta_l = 65.7;
Exglobal_u = Ex*cosd(theta_u)+Ez*sind(theta_u);
Ezglobal_u = Ez*cosd(theta_u)+Ex*sind(theta_u);
Exglobal_l = Ex*cosd(theta_l)+Ez*sind(theta_l);
Ezglobal_l = Ez*cosd(theta_l)+Ex*sind(theta_l);

Error using input
Cannot call INPUT from EVALC.

Error in laminate_properties (line 42)
layup= input('Which layup do you want to use
(Ibeam_web(1),Ibeam_flange(2),rect_sides(3),rect_tb(4))');

```

Published with MATLAB® R2015a

```

%Calculation of laminate properties
clear all
close all
clc

%Constants
h=43E-3;
b=56E-3;

%I-beam
%Constants
h1=35.8E-3;
h2=3.6E-3;
b1=1.8E-3;
core=5E-3;
b2=47.4E-3/2;
y=28E-3;
Ex_flange = 70.6544;
Ex_web=70.6544;
E_core=0.18;

EI_ibeam = Ex_flange*(((b*(h1+2*h2)^3)/12) -
  Ex_flange*((b*(h1)^3)/12)+ Ex_web*((2*b1*(h1)^3)/12) +
  E_core*((core*(h1)^3)/12)

%Rectangular
H1=32.2E-3;
H2=5.4E-3;
B1=50E-3;
B2=3E-3;
Y=28E-3;
Ex_sides=66.9709;
Ex_tb= 64.3755;

EI_rect = Ex_tb*((b*(H1+2*H2)^3)/12) - Ex_tb*((b*(H1)^3)/12) +
  Ex_sides*((2*B2*(H1)^3)/12)

EI_ibeam =

    1.2063e-05

EI_rect =

    1.4974e-05

```

Published with MATLAB® R2015a

C.

Calculations after four point bending test

The maximum obtained strain and load capacity of the joiners obtained during the four point bending test, were used to calculate the moment in the middle of each structure. To find the bending stiffness, this moment were used. The following sections show the calculations.

The free body diagram of the four point bending test, are shown in Figure C.1. Where F represent the maximum applied load.

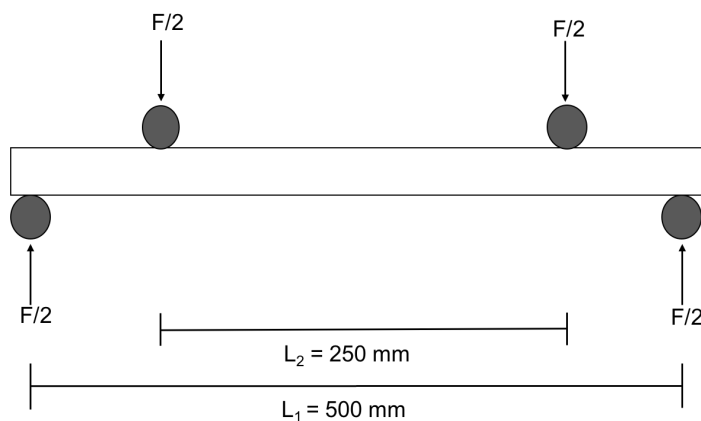


Figure C.1: Free body diagram

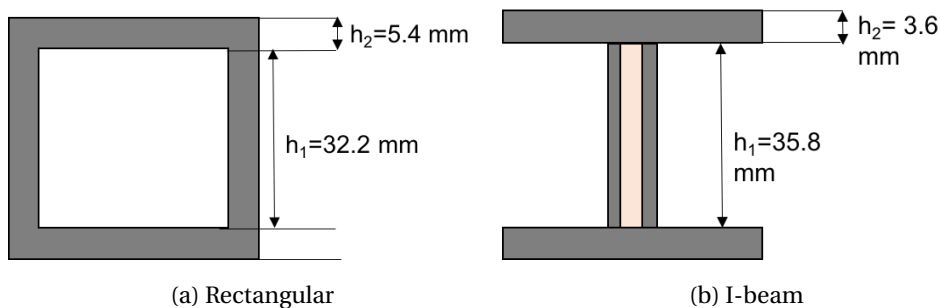


Figure C.2: Geometric dimensions

From the free body diagram the equation for the moment are given by:

$$M = \frac{F}{4}(L_1 - L_2) \quad (\text{C.1})$$

From Equation 2.9 and Equation 2.12, the moment could be written as:

$$M = EI \frac{\epsilon_{max}}{\frac{h_1}{2} + h_2} \quad (\text{C.2})$$

Then the bending stiffness could be found by:

$$EI = \frac{M(\frac{h_1}{2} + h_2)}{\epsilon_{max}} \quad (\text{C.3})$$

C.1 Rectangular box profile

For the rectangular box profile, using equations C.1-C.3, and the measured values for the maximum load capacity and strain, the moment and bending stiffness were calculated as shown below.

$$F = 34.33 \text{ kN}, \epsilon_{\max} = 2.592 \times 10^{-3}$$

$$M = \frac{F}{4}(L_1 - L_2) = \frac{34.33 \text{ kN}}{4}(500 \times 10^{-3} \text{ m} - 250 \times 10^{-3} \text{ m}) = 2.14 \text{ kNm}$$

$$EI = \frac{M(\frac{h_1}{2} + h_2)}{\epsilon_{max}} = \frac{2.14 \text{ kNm}(\frac{32.2 \times 10^{-3} \text{ m}}{2} + 5.4 \times 10^{-3} \text{ m})}{2.592 \times 10^{-3}} = 17.75 \text{ kNm}^2$$

C.2 I-beam

For the I-beam, using equations C.1-C.3, and the measured values for the maximum load capacity and strain, the moment and bending stiffness were calculated as shown below.

$$F = 36.01 \text{ kN}, \epsilon_{\max} = 4.224 \times 10^{-3}$$

$$M = \frac{F}{4}(L_1 - L_2) = \frac{36.01 \text{ kN}}{4}(500 \times 10^{-3} \text{ m} - 250 \times 10^{-3} \text{ m}) = 2.25 \text{ kNm}$$

$$EI = \frac{M(\frac{h_1}{2} + h_2)}{\epsilon_{\max}} = \frac{2.25 \text{ kNm}(\frac{35.8 \times 10^{-3} \text{ m}}{2} + 3.6 \times 10^{-3} \text{ m})}{4.224 \times 10^{-3}} = 11.45 \text{ kNm}^2$$

D. Risk Assessment

NTNU	Kartlegging av risikofylt aktivitet			Utarbeidet av	Nummer	Dato	
HMS				HMS-avd.	HMSRV/2601	22.03.2011	
		Godkjent av		Erstatter			
		Rektor		01.12.2006			

Enhet: Institutt for Produktutvikling og Materialer, Laboratorie for Polymerer og Kompositter

Dato: 14.01.2016

Linjeleder: Torgeir Welo

Deltakere ved kartleggingen (m/ funksjon): Sigrd Moen, Nils Petter Vedvik
(Ansv. veileder, student, evt. medveileder, evt. andre m. kompetanse)

Kort beskrivelse av hovedaktivitet/hovedprosess: Masteroppgave Sigrd Moen

Er oppgaven rent teoretisk? NEI

«JA»: Beskriv kort aktiviteten i kartleggingskjemaet under. Risikovurdering trenger ikke å fylles ut. «JA» betyr at veileder innestår for at oppgaven ikke inneholder noen aktiviteter som krever risikovurdering. Dersom

Signaturer: Ansvarlig veileder: 

Student: 

ID nr.	Aktivitet/prosess	Ansvarlig	Eksisterende dokumentasjon	Eksisterende sikrings tiltak	Lo, forskrift o.l.	Kommentar
1	Blanding av Epoxy	Sigrd Moen	Sikkerhetsdatablad	Vernebriller, hansker, avtrekk	Arbeidsmiljøloven, Kjemikalieforskriften, Lab- og verkstedshåndboken NTNU	
2	Påføring av Epoxy	Sigrd Moen	Sikkerhetsdatablad	Vernebriller, hansker, avtrekk	Arbeidsmiljøloven, Kjemikalieforskriften, Lab- og verkstedshåndboken, NTNU	
3	Mekanisk testing	Sigrd Moen	Romoppføring, HMS-kurs	Vernebriller, hørsevern	Arbeidsmiljøloven, Lab- og verkstedshåndboken, NTNU	

NTNU	 Risikovurdering			Utarbeidet av	Nummer	Dato
				HMS-avd.	HMSRV2601	22.03.2011
HMS				Godkjørt av		Erslatter
		Rektor		01.12.2006		

Sannsynlighet vurderes etter følgende kriterier:

Svært liten 1	Liten 2	Middels 3	Stor 4	Svært stor 5
1 gang pr 50 år eller sjeldnere	1 gang pr 10 år eller sjeldnere	1 gang pr år eller sjeldnere	1 gang pr måned eller sjeldnere	Skjer ukentlig

Konsekvens vurderes etter følgende kriterier:


Gradering	Menneske	Ytre miljø Vann, jord og luft	Øk/materiell	Omdømme
E Svært Alvorlig	Død	Svært langvarig og ikke reversibel skade	Drifts- eller aktivitetsstans > 1 år.	Troverdighet og respekt betydelig og varig svekket
D Alvorlig	Alvorlig personskade. Mulig uførhet.	Langvarig skade. Lang restitusjonstid	Driftsstans > ½ år Aktivitetsstans i opp til 1 år	Troverdighet og respekt betydelig svekket
C Moderat	Alvorlig personskade.	Mindre skade og lang restitusjonstid	Drifts- eller aktivitetsstans < 1 mnd	Troverdighet og respekt svekket
B Liten	Skade som krever medisinsk behandling	Mindre skade og kort restitusjonstid	Drifts- eller aktivitetsstans < 1uke	Negativ påvirkning på troverdighet og respekt
A Svært liten	Skade som krever førstehjelp	Ubetydelig skade og kort restitusjonstid	Drifts- eller aktivitetsstans < 1dag	Liten påvirkning på troverdighet og respekt

Risikoverdi = Sannsynlighet x Konsekvens

Beregn risikoverdi for Menneske. Enheten vurderer selv om de i tillegg vil beregne risikoverdi for Ytre miljø, Økonomi/materiell og Omdømme. I så fall beregnes disse hver for seg.

Til kolonnen "Kommentarer/status, forslag til forebyggende og korrigerende tiltak":

Tiltak kan påvirke både sannsynlighet og konsekvens. Prioriter tiltak som kan forhindre at hendelsen inntreffer, dvs. sannsynlighetsreducerende tiltak foran skjerpet beredskap, dvs. konsekvensreducerende tiltak.

NTNU		Risikomatrixe		Dato	
				08.03.2010	
HMS/KS				Erstatter	
		utarbeidet av		Nummer	
		HMS-avd.		HMSRV2604	
		godkjent av			
		Rektor		09.02.2010	



MATRISSE FOR RISIKOVURDERINGER ved NTNU

KONSEKVENSENS	Svært alvorlig	E1	E2	E3	E4	E5
	Alvorlig	D1	D2	D3	D4	D5
	Moderat	C1	C2	C3	C4	C5
	Liten	B1	B2	B3	B4	B5
	Svært liten	A1	A2	A3	A4	A5
		Svært liten	Liten	Middels	Stor	Svært stor
SANNSYNLIGHET						

Prinsipp over akseptkriterium. Forklaring av fargene som er brukt i risikomatrixen.

Farge	Beskrivelse
Rød	Uakseptabel risiko. Tiltak skal gjennomføres for å redusere risikoen.
Gul	Vurderingsområde. Tiltak skal vurderes.
Grønn	Akseptabel risiko. Tiltak kan vurderes ut fra andre hensyn.